Technische Universität München

TUM School of Life Sciences

Lehrstuhl für Bodenkunde

Elucidation of Phosphorus Cycling in Temperate Forest Ecosystems by Synchrotron-based X-ray Absorption Spectroscopy

Luis Carlos Colocho Hurtarte

Vollständiger Abdruck der von der TUM School of Life Sciences der Technischen Universität München zur Erlangung
des akademischen Grades eines

Doktors der Naturwissenschaften

genehmigten Dissertation.

Vorsitzende: Prof. Dr. Anja Rammig

Prüfer der Dissertation:

1. apl. Prof. Dr. Jörg Prietzel

2. Prof. Dr. Dr. h.c. Ingrid Kögel-Knabner

3. Prof. Dr. Wulf Amelung

Die Dissertation wurde am 27.05.2021 bei der Technischen Universität München eingereicht und durch die TUM School of Life Sciences am 29.09.2021 angenommen.

Para mi Papá, quien vive a través de mi

"Study hard what interests you the most in the most undisciplined, irreverent, and original manner possible."

— Richard Feynmann

I Summary

Phosphorus (P) stands out as a central element for the functioning of terrestrial ecosystems, with its soil speciation being a key factor for P bioavailability. However, at present it is not clear how soil P speciation is affected by different climate conditions, nor how microspatial soil P distribution and speciation patterns are shaped by plant roots. Temperate forests stand out as ecosystems whose P availability strongly affects forest vitality and productivity. Therefore, it is of pivotal importance to understand the P dynamics in these ecosystems. Synchrotron-based X-ray spectroscopy and microspectroscopy allow soil P analyses including P speciation at the macro- and the microscale to help answering these questions. However, particular characteristics of the element phosphorus, like its low concentration in soils and the fact that the analysis of P X-ray spectra is not straightforward, complicate the application of synchrotron-based X-ray spectroscopy and microspectroscopy for soil P analysis. In addition, current approaches to investigate interactions between the biosphere and the soil with relevance for ecosystem P cycling at the microscale level are prone to methodological artefacts during sample preparation. This thesis aimed to contribute to answer the above-mentioned questions by developing, optimizing, and applying novel synchrotron-based X-ray (micro)spectroscopy methods for soil P analysis at the macro- and micro-scale.

The objectives of this thesis were approached through three main projects:

1. **Improvement of synchrotron-based X-ray spectroscopy methods for the analysis of phosphorus in soils.** The speciation of phosphorus in soils is critical to understand its turnover and dynamics in terrestrial ecosystems. Therefore, one important goal of this thesis was to optimize current synchrotron-based P K-and $L_{2,3}$-edge XANES spectroscopy methods in order to achieve a most correct (i.e. precise and accurate) quantification of different organic and inorganic P species in soils. Here, I developed important workflows for a correct analysis of phosphorus in soils and other materials, with broad applications in environmental sciences.

2. **Synoptic investigation of concomitant C, N, P, and S speciation changes in mountain forest soils across a temperature gradient.** Aware of the great power of combined XANES and NMR spectroscopy for the analysis and speciation of carbon (C), nitrogen (N), P, and sulfur (S) in soils, I investigated the influence of a temperature gradient on the C, N, S and P speciation in a mountain forest soil with a synoptic approach. Additionally, I combined these chemistry-focussed studies with microbiological analyses (soil microbial bio- and necromass, community composition, enzymatic activity). This comprehensive approach enabled me to discern the dynamic changes in soil P speciation (from

organic P-dominated to inorganic P-dominated) and soil N speciation (from protein-N-dominated to heterocyclic N-dominated) as a product of microbial succession in the temperature gradient.

3. **Evaluating the influence of soil phosphorus speciation and soil mineral composition on the root functionality of *Picea abies* L. seedlings and associated microspatial distribution patterns of C and P in silicate and calcareous soils.** Motivated by the observation of organic P accumulation in temperate forest soils, I aimed to understand the processes responsible for the organic P accrual. I produced artificial soils with contrasting initial soil P speciation (organic *vs.* inorganic P) and mineral composition (silicate- *vs.* dolomite-based), and cultivated *Picea abies* L. seedlings on microcosms containing the different soil variants in a two-factorial experiment with respect to soil P form and mineral composition. I was able to unravel the plasticity of important root traits and effects on microspatial soil P distribution and speciation patterns in the different experimental variants.

In *Studies 1a and 1b*, both assigned to Project 1, I developed two novel approaches for soil P analysis using XANES spectroscopy. *Study 1a* reveals the shortcomings of P K-edge XANES for the investigation of soil samples with high P concentrations, and highlights the use of new computational tools to minimize analytical errors for such soils. *Study 1b* presents a novel method for the deconvolution of P $L_{2,3}$-edge XANES spectra, which allows a better quantification of organic P species in soils and other environmental materials.

The findings of *Study 2*, assigned to Project 2, revealed the concomitant changes of SOC, N, S, and P stocks and speciation in forest soils across a temperature gradient. At a lower temperature (forest dominated soils), SOC was mostly lignin-associated, N was mostly protein-associated, and P was mostly organically bound, while at a higher temperature (alpine meadow-dominated soil), SOC-lignin, N-protein and organic P were largely decomposed, associated with an accrual of SOC-lipids, heterocyclic N, and inorganic P. These processes could not have been identified by any single soil analysis, but only by their combination. Thus, my combined approach has been shown to be of fundamental importance for the analysis of abiotic disturbance impacts on C and nutrient cycling in temperate forest ecosystems.

The findings of *Study 3*, assigned to Project 3, revealed that the initial soil P speciation modulates functional root traits expressed by plants, inducing different C, N and P dynamics in soils. Roots of *Picea abies* L. seedlings grown in inorganic P-rich soils were thinner and longer than roots of *Picea abies* L. seedlings grown in soils that were rich in organic P, but otherwise identical. This led to a higher SOC accumulation in the soils with inorganic P compared to

those with organic P. However, at the microscale, in the organic P soil, regions with particular P enrichment were also zones with particular enrichment of organic C. Thus, fine-scale microspatial analysis suggests that root-microbial association and cooperation is more important for the acquisition of organic P than for inorganic P by plants, independent of soil mineralogy. Here I demonstrate the importance of microscale spatial soil analysis to reveal key processes of plant P acquisition from soils.

Overall, this thesis is innovative by providing important and novel methodological approaches for the investigation of P in soils at the microscale and the macroscale. It also demonstrates the important, yet so far often underestimated role of organically bound soil phosphorus in regulating plant P availability in terrestrial ecosystems.

II Zusammenfassung

Phosphor (P) ist ein zentrales Element für das Funktionieren terrestrischer Ökosysteme, und die P-Bindungsformenverteilung im Boden gilt als Hauptfaktor für seine Bioverfügbarkeit. Es ist jedoch momentan noch ungeklärt, inwieweit die P-Bindungsformen in Böden durch unterschiedliche Klimabedingungen beeinflusst wird und wie die kleinräumigen Muster der Boden-P-Verteilung und P-Speziierung durch Pflanzenwurzeln geformt werden. In diesem Kontext sind Wälder gemäßigter Klimate in besonderem Maße dadurch charakterisiert, dass ihre Vitalität und Produktionskraft entscheidend durch die P-Verfügbarkeit beeinflusst ist. Daher ist es von entscheidender Bedeutung, die P-Dynamik dieser Ökosysteme zu verstehen. Synchrotron-basierte röntgenspektroskopische und röntgenmikrospektroskopische Methoden ermöglichen Boden-P-Analysen einschließlich einer P-Speziierung sowohl auf der Makro- als auch auf der Mikroskala, um diese Fragen zu beantworten. Besondere Eigenschaften des Elements Phosphor sind in diesem Zusammenhang seine in Böden meist geringe Konzentration sowie die Tatsache, dass die Analyse von P-Röntgenspektren oftmals kompliziert ist. Dies schränkt gegenwärtig die Anwendung Synchrotron-basierter röntgenspektroskopischer Methoden in der Boden-P-Forschung stark ein. Darüber hinaus sind aktuelle Ansätze zur mikroskaligen Untersuchung von Wechselwirkungen zwischen Biosphäre und Boden mit Relevanz für den P-Kreislauf in terrestrischen Ökosystemen aufgrund der komplexen Probenvorbereitung anfällig für methodische Artefakte. Diese Arbeit zielte darauf ab, durch Optimierung und Anwendung neuartiger Synchrotron-basierter röntgen-(mikro)spektroskopischer Methoden für die Analyse von P in Böden auf der Makro- und der Mikroskala einen Beitrag zur Beantwortung der oben genannten Fragen zu leisten.

Die Ziele dieser Arbeit wurden durch drei Hauptprojekte erreicht:

1. Verbesserung Synchrotron-basierter röntgenspektroskopischer Methoden für die Analyse von Phosphor im Boden. Die analytische Speziierung von Phosphor in Böden ist entscheidend für das Verständnis seines Umsatzes und seiner Dynamik in terrestrischen Ökosystemen. Daher bestand ein wichtiges Ziel dieser Arbeit darin, in den letzten Jahren etablierte Methoden der Synchrotron-basierten P K- und $L_{2,3}$-Kanten-XANES-Spektroskopie im Hinblick auf eine möglichst korrekte, d.h. präzise und akkurate Quantifizierung verschiedenartiger organischer und anorganischer P-Spezies in Böden zu optimieren. Hier entwickelte ich wichtige Protokolle („Workflows“) für die korrekte Analyse von Phosphor mit einem breitem Anwendungsspektrum in der Umweltwissenschaft.

2. Synoptische Untersuchung synchroner Veränderungen der C-, N-, P- und S-Bindungs formen in Gebirgswaldböden im Verlauf eines Temperaturgradienten. Im Bewusstsein der großen analytischen Kraft kombinierter XANES- und NMR-spektroskopischer Methoden für die Analyse und Speziierung von Kohlenstoff (C), Stickstoff (N), P und Schwefel (S) in Böden nutzte ich eine derartige Kombination zur Untersuchung des Einflusses eines Temperaturgradienten auf die Bindungsformenverteilung von C, N, S und P in einem Gebirgswaldboden in einem synoptischen Ansatz. Diesen chemisch-analytischen Ansatz kombinierte ich zusätzlich mit mikrobiologischen Analysen (mikrobielle Bio- und Nekromasse, Zusammensetzung der Mikroorganismen gemeinschaft, Aktivitäten wichtiger Enzyme). Mit Hilfe dieses umfassenden Ansatzes konnte ich eine dynamische Bindungsformenänderung des im Boden gebundenen P (von P_{org}-dominiert zu P_{anorg}-dominiert) und N (von Protein-dominiert zu heterocyclisch-N dominiert) als Produkt einer mikrobiellen Sukzession unter dem Einfluss des Temperaturgradienten nachweisen.

3. Bewertung des Einflusses von initialer Boden-P-Speziierung und Bodenmineral-ausstattung auf die Wurzelfunktionalität von Fichten- (*Picea abies* L.*)* Sämlingen und dadurch hervorgerufene kleinräumige Verteilungsmuster von C und P in Silikat- und Carbonatböden. Motiviert durch meine Beobachtungen der Anreicherung von organisch gebundenem P in Waldböden der gemäßigten Klimazone wollte ich die für diese Anreicherung maßgeblichen Prozesse besser verstehen. Ich produzierte „künstliche Böden" mit kontrastierender initialer P-Speziation (ausschließlich organisch *vs.* anorganisch gebundener P) und Mineralausstattung (silikatisch *vs.* dolomitisch) und kultivierte in einem zweifaktoriellen Versuchsdesign (Faktoren: P-Bindungsform, Mineralausstattung) Fichten- *(Picea abies* L.*)*-Sämlinge in Mikrokosmen der verschiedenartigen Bodenvarianten. Ich konnte so die Plastizität von Wurzelmerkmalen und ihre Auswirkungen auf kleinräumige Verteilungsmuster von C und P sowie der P-Bindungsformen in den Böden der unterschiedlichen Versuchsvarianten aufdecken.

In *Studie 1a* und *1b* (beide erstellt in Projekt 1) entwickelte ich zwei neuartige Ansätze für die P-Analyse in Böden mittels XANES-Spektroskopie. *Studie 1a* verdeutlicht die gegenwärtigen Mängel von P K-Kanten XANES bei der Analyse von Böden mit hohen P-Konzentrationen und beschreibt neuentwickelte Auswerteverfahren zur Minimierung von Analysefehlern. In *Studie 1b* wird eine neue Methode zur Analyse von P $L_{2,3}$-Kanten-XANES-Spektren vorgestellt, die eine bessere Quantifizierung organischer P-Spezies in Böden und anderen Materialen ermöglicht.

Die Ergebnisse von *Studie 2* (erstellt in Projekt 2) beschreiben die synchronen Veränderungen der Vorräte und Bindungsformen von SOC, N, S und P in Waldböden über einen Temperaturgradienten. Bei einer niedrigeren Temperatur (vom Wald dominierte Böden) war der SOC größtenteils mit Lignin assoziiert, der N war proteindominiert und der P war größtenteils organisch gebunden, während bei einer höheren Temperatur (angrenzende, zunehmend von Almwiese dominierte Böden) SOC-Lignin-, N-Protein- und organische P-Verbindungen stark um- bzw. (P) abgebaut waren. Dieser Prozess war mit einer Akkumulation von SOC-Lipiden, hetero-cyclischem N und anorganischem P im Boden verbunden. Diese Prozesse hätten nicht anhand einzelner spezifischer Bodenuntersuchungen ermittelt werden können, sondern nur mittels der angewendeten Kombination sämtlicher Methoden. Der in Studie 2 eingesetzte kombinierte Ansatz erwies sich somit als von grundlegender Bedeutung für die Analyse und Bewertung der Auswirkungen abiotischer Störungen auf den C- und Nährstoffkreislauf in Wäldern der gemäßigten Klimazone.

Die Ergebnisse von *Studie 3* (erstellt in Projekt 3) zeigten, dass die ursprüngliche Boden-P-Bindungsform die exprimierten funktionellen Wurzelmerkmale von Pflanzen moduliert, was zu einer unterschiedlichen C-, N- und P-Dynamik in hinsichtlich ihrer initialen P-Ausstattung verschiedenartigen Böden führt. Die Wurzeln der in den mit anorganischem P versetzten Böden gezogenen Fichtensämlinge waren dünner und länger als jene der Fichtensämlinge, die in mit organisch gebundenem P versetzten, aber sonst identischen Böden gezogen waren. Dies war mit einer stärkeren SOC-Anreicherung in den mit anorganischem P versetzten Böden verbunden. Auf der Mikroskala waren die P-Anreicherungszonen der mit organisch gebundenem P versetzten Böden auch Zonen mit erhöhten SOC-Gehalten. Mittels der feinskaligen kleinräumigen Analyse konnte ich zeigen, dass räumliche Assoziation bzw. Kooperation von Wurzeln und Bodenmikro-organismen bei der Aufnahme von organisch gebundenem Boden-Phosphor durch Pflanzen offenbar sowohl in silikatischen als auch in dolomitischen Böden eine wichtigere Rolle spielt als bei der Pflanzenaufnahme von anorganischem P. Hier demonstriere ich die große Bedeutung mikroskaliger Bodenanalyseverfahren für die Aufklärung von Schlüsselprozessen der P-Aufnahme von Pflanzen aus Böden.

Insgesamt ist diese Arbeit einerseits dadurch innovativ, dass sie wichtige und neuartige methodische Ansätze für die Untersuchung von in Boden gebundenem P sowohl auf der Mikroskala als auch auf der Makroskala präsentiert. Des Weiteren demonstriert sie die bislang oftmals noch unterschätzte Rolle des organisch im Boden gebundenen Phosphors bei der Regulierung der Verfügbarkeit von P in terrestrischen Ökosystemen.

III Acknowledgement

I dedicate this thesis to my father, Jose Luis Colocho Ortega, losing him was the hardest punch life has given me. Yet, through all my friends and family, I overcame and climbed through. He, who never gave up, whom I admired the most, is helping me even now. I also share this success with my Mother and my sister who have always supported me.

When I look back through this thesis, I see many individuals that helped me, academically and personally. None of them come close to what Prof. Jörg Prietzel did for me. I am very grateful for entrusting me with this project and recognizing my enthusiasm for science and synchrotrons. I consider him my college and my friend and I am deeply thankful for looking at me early in 2012 and seeing my potential. Furthermore, I am deeply in debt with Dr. Peter Schad, who let me come in 2012 as a student here and let me participate in the soil excursions.

My time at the Chair was also supported by Prof. Ingrid Koegel-Knabner, who has my admiration and most gratefulness. The DFG is also kindly acknowledged for financial support. Moreover, all my work has was built with the help of many co-authors, without whom the outcome would not have been successful. I especially thank Dean Hesterberg, Helen Amorim, Julio Crzinski, Wulf Amelung, Liming Wang, Sabine Wiebold, Ellen Kandeler, Thomas Huthwelker, Reto Wetter, Camelia Borca, Steffen Schweizer, Svenja Müller, and Dingzhu Liao. My co-authors' work is only partially eclipsed by the work of the technicians, specially: Sigrid, Gerti, Franzi Fella, and Maria. Besides that, I would like to acknowledge the help from Gabi, Petra Bucher, Baerbel, Michaela, Hans, Christine, Marzena, and Florian on the day-to-day duties.

During these years my life revolved around work, and it was easy with such great colleges as the Chair of Soil Science. I am deeply grateful for my friends from the 2012 exchange who were still here Florian Werner (the saddest part is us not having the opportunity to work together), Lydia Paetsch, and Meike. Later on, I bounded with the new "Ph. D. gang", I especially thank Chris, Julien, and Siwei-Luo for the nice stories and time together. Furthermore, I was lucky enough to share my time at the BOKU with the greatest Ph.D. colleagues (Franzi Bucka, Evelin, Tianyi, Kristina, Franzi Steiner, Thiago, and Alix). I have been fortunate to share my time here with Brazilian colleagues (Luis Bola and Pedro), which made my time here funnier and more balanced.

On a personal level, I have been rewarded with lasting friendships. I am deeply thankful for the help from Michi, Maike, Johnny, Anne Kindermann, and Thomas Alsruth, Rodrigo and Alefe. Last year, I was awarded the help and support of my dear Noelia, whose lively approach to life helps me balance and grow as a scientist and as a person.

To all others that crossed my path, many thanks!

IV List of Studies

This dissertation is based on the following first-authored and co-authored research studies. All first-authored studies are attached in appendices A – D.

Study Ia	
Title	Optimization of Data Processing Minimizes Impact of Self-Absorption on phosphorus Speciation Results by P K-Edge XANES
Authors	**Colocho Hurtarte, L.C.**, Souza-Filho, L.F., Santos, W.O., Vergütz, L., Prietzel, J., Hesterberg, D.
Publication	Soil Systems 3 (2019), 61. 10.3390/soilsystems3030061
Objectives	Determine the optimal concentration of P to collect XANES spectroscopy data in fluorescence mode. Investigate if recent improvements in data processing optimization may also improve the LC fitting results even when self-absorption is present.
Results and Discussion	We produced a series of ternary standard mixtures (calcium-iron-aluminum phosphates) and an example soil sample both diluted using boron nitride over a range from 1 to ~900 mmol kg^{-1} for the soil sample and up to ~6000 mmol kg^{-1} for the standard mixtures. We show that by optimizing background subtraction and normalization values, consistent results with <10% error can be obtained for samples containing up to 300 mmol kg^{-1} P.
Contributions	Leading data analysis and discussion, writing and revision of manuscript with input from co-authors

Study Ib	
Title	A Novel Approach for the Quantification of Different Inorganic and Organic Phosphorus Compounds in Environmental Samples by P $L_{2,3}$ -Edge X-ray Absorption Near-Edge Structure (XANES) Spectro-scopy
Authors	**Colocho Hurtarte, L.C**., Santana Amorim, H.C., Kruse, J., Criginski Cezar, J., Klysubun, W., Prietzel, J.
Publication	Environmental Science & Technology 54 (2020) 2812-2820. 10.1021/acs.est.9b07018
Objectives	Develop a protocol for the quantification of different organic and inorganic P species in soils using synchrotron-based X-ray absorption near-edge structure (XANES) spectroscopy at the P $L_{2,3}$-edge. Compare its accuracy and precision to other P speciation methods.
Results and Discussion	The protocol for quantification was developed and incorporated into our R package. We evaluated the accuracy and precision by analyzing 40 standard mixtures composed of seven different inorganic and organic P compounds (with a mean of $R^2 = 0.85$). Using the P $L_{2,3}$-edge, we identified different organic P species, including those not identified by the common P K-edge XANES. However, there is a consistent underestimation of organic polyphosphates. Overall, the application of P $L_{2,3}$-edge XANES provides a higher level of information than by P K-edge XANES, although the ubiquitous use of this novel methodology is still limited to samples with a phosphorus content above 3 mg g^{-1}.
Contributions	Leading experimental design, data acquisition and analysis, and discussion, writing and revision of manuscript with input from co-authors

Study II	
Title	Quantifying Molecular-level Soil Organic Matter Changes in Temperate Mixed Mountain Forests in Response to Climate Warming
Authors	**Colocho Hurtarte, L.C.,** Mueller, S., Wang, L., Kandeler, E., Amelung, W., Willbold, S., Thieme, J., Jaye, C., Fischer, D., Klysubun, W., Prietzel, J.
Publication	Global Change Biology – Under Review
Objectives	Investigate the relationship between changes in the molecular composition of soil organic carbon (SOC), N, P, and S, microbial community necromass and composition, and soil enzymatic activity.
Results and Discussion	We observed that temperature increases are accompanied by lower SOC content, yet no visible shifts in nutrient content. On the other hand, fungal biomass increased and gram-negative bacteria decreased along the gradient. These shifts in microbial community composition were accompanied by decreases in phenol oxidase and acid monoester phosphatase activities and increases in leucine peptidase activities. Our multi-spectroscopy data unravel the preferential depletion of lignin, amino peptides, and monoester phosphates for the formation of microbial biomass and the accumulation of heterocyclic N, sulfate, and inorganic phosphate. These findings indicate that under increasing temperature and decreasing C input, microbial turnover increases, and the remaining communities are preferentially shifted towards those that thrive under strained C and nutrient input.
Contributions	Analysis of all data (partially based on previously unpublished results), additional ^{31}P and ^{13}C NMR measurements, writing and revision of manuscript with input from co-authors

Study III	
Title	Functional plasticity shapes patterns of phosphorus acquisition in temperate forests
Authors	**Colocho Hurtarte L. C.** , Liao D., Schweizer S., Müller S., Araki T., Wetter R. , Borca C., Huthwelker T., Klingl A., Prietzel J.
Publication	In preparation
Objectives	Investigate the effect of initial soil P speciation on root functional traits and microspatial soil C and P distribution on *Picea abies* L. seedlings.
Results and Discussion	We observed that the initial P speciation modulates the root functional traits expressed by *Picea abies* L. seedlings. While SOC increased in the inorganic P variant, the microspatial association of C and P was higher. This difference in microspatial co-localization shows the different mechanisms for P acquisition utilized in each variant, which are highly dependent on root/microbial associations in the organic P-rich soils, and less so in inorganic P-rich soils. We show for the first time, by analysing the P dynamics at the microscale, direct evidence of the P internal cycling in temperate forests.
Contributions	Analysis of all data, experiment execution, cryo-sample design and testing.

V Co-authored studies

Study I	
Title	Site conditions and vegetation determine phosphorus and sulfur speciation in soils of Antarctica.
Authors	Prietzel, J., Prater, I., **Colocho Hurtarte, L.C.**, Hrbáček, F., Klysubun, W., Mueller, C.W.
Publication	Geochimica et Cosmochimica Acta 246, 339–362. doi:10.1016/j.gca.2018.12.001
Contribution	Support in synchrotron data acquisition and analysis. Statistical data analysis. Joint interpretation of results.

Study II	
Title	The fate of calcium in temperate forest soils – A Ca K-edge XANES study
Authors	Prietzel, J., Klysubun, W., **Colocho Hurtarte, L.C.**
Publication	Biogeochemistry 152(2), 195-222. doi:10.1007/s10533-020-00748-6
Contribution	Support in synchrotron data discussion and joint interpretation of results. Development and visualization of a conceptual model of pedogenetical Ca speciation change in calcareous soils.

Study III	
Title	Calcium speciation in limed Brazilian Oxisols Using Ca K-edge XANES spectroscopy
Authors	Hesterberg, D., Teixeira, W., **Colocho Hurtarte, L. C.**, Vergutz, L., de Souza Filho, L. F., Alvarez Venegas, V. H.
Publication	Geoderma – Submitted
Contribution	Support in synchrotron data analysis and joint interpretation of results.

Study IV	
Title	Fate of phosphorus as determined by chemical fractionation and P K-edge XANES in long-term cultivated Brazilian soils
Authors	Viera dos Reis, J., Hesterberg, D., **Colocho Hurtarte, L. C.**, Muraoka, T.
Publication	Plant and Soil – Submitted
Contribution	Support in synchrotron data analysis and joint interpretation of results.

Study V	
Title	Biotic and abiotic controls on Carbon storage in aggregates in calcareous alpine and pre-alpine grassland soils
Authors	Garcia Franco, N., Warter, R., Wiesmeier, M., **Colocho Hurtarte, L. C.**, Berauer, B. J., Buness, V., Zistl-Schlingmann, M., Kiesse, R., Dannenmann, M., Kögel-Knabner, I.
Publication	Biology and Fertility of Soils 57, 203–218 (2021). https://doi.org/10.1007/s00374-020-01518-0
Contribution	Support in data analysis and interpretation of results.

Study VI	
Title	Phosphorus removal from aqueous solution using cation-modified biochars: speciation using P K-edge XANES spectroscopy
Authors	Nardis, B. O., Barbosa, C. F., Silva Penido, E., Hesterberg, D., **Colocho Hurtarte, L. C.**, Guimarães Guilherme, L. R., Azevedo Melo, L.C.
Publication	Chemosphere – Submitted
Contribution	Support in synchrotron data analysis, SEM-EDX measurements and interpretation of results.

Study VII	
Title	Forest litter constraints on the pathways controlling soil organic matter formation
Authors	Almeida, L. F. J., **Colocho Hurtarte, L. C.**, Teixeira, P.P., Inagaki, T. M., Souza, I. F., da Silva, I. R., Mueller C. W.
Publication	Global Change Biology – Submitted
Contribution	Joint sample analysis and interpretation of the results.

Study VIII	
Title	Lead Speciation and Availability Affected by Plants in a Contaminated Soil
Authors	Santana Amorim, H. C., **Colocho Hurtarte, L. C.**, Vergütz, L., Ribeiro Silva, I., Vinhas Costa, O., Pacheco, A., Fontes, M.
Publication	Environmental Science and Technology – Submitted
Contribution	Support in synchrotron data analysis, and interpretation of results.

Study IX	
Title	Pruning residues incorporation and reduced tillage improve soil organic matter stabilization and structure of salt-affected soils in a semi-arid Citrus tree orchard
Authors	Garcia-Franco, N., Wiesmeier, M., **Colocho Hurtarte, L. C.**, Fella, F., Martínez-Mena, M., Almagro, A., García Martínez, E., Kögel-Knabner, I.
Publication	Soil & Tillage – In review
Contribution	Support in data analysis and interpretation of results

Table of Contents

VI List of Abbreviations

Al	Aluminium
ATP	Adenosine Triphosphate
C or ^{13}C	Carbon
Ca	Calcium
DNA	Deoxyribonucleic Acid
E_0	Edge energy
EDTA	Ethylenediamine tetraacetic Acid
Fe	Iron
FID	Flame Ionization Detector
FY	Fluorescence Yield
GC	Gas Chromatograph
HSQC	Heteronuclear Single Quantum Coherence Spectroscopy
HydAp	Hydroxyapatite
HF/$HClO_4$	Hydrofluoric acid/perchloric acid
ICP-OES	Inductively Coupled Plasma-Optical Emission Spectroscopy
IHP	Inositol hexakisphosphate
LCF	Linear combination fitting
MAS	Magic Angle Spinning
MDPA	Methylene Diphosphonic Acid
N	Nitrogen
NaOH	Sodium Hydroxide
NLFA	Neutral Lipid Fatty Acids
NMR	Nuclear Magnetic Resonance Spectroscopy
P or ^{31}P	Phosphorus
Phos	Phosphonate
PO_4^{3-}	orthophosphate or inorganic P
PC	Phosphatidylcholine
PEY	Partial electron yield
PLFA	Phospholipid Fatty Acids
ppm	Parts per million

RNA	Ribonucleic Acid
S	Sulfur
SDD	Silicon-drift detector
SEM	Scanning electron microscope
SLRI	Synchrotron Light Research Institute
SOM	Soil organic matter
TCP	Tribasic calcium phosphate
XANES	X-ray Absorption Near-Edge Structure Spectroscopy
XRF	X-ray fluorescence

1. Introduction

1.1 The terrestrial cycle of phosphorus

Our concept of life is based on organisms that use phosphorus (P) in all stages of their development. In terrestrial environments, P is predominantly present as the molecule orthophosphate (PO_4), either isolated or bound to various biomolecules, whose functions range from energy transport to serving as a structural component in cell walls and nucleic acids (Elser et al., 2007). Life as we know could not exist without this element (Bennet and Elser, 2009; Elser, 2012). Thus, imposing a limit to an organism on its P acquisition/nutrition interferes with its development, and on the ecosystem level limits primary productivity. Studies that aim to understand the dynamics of elements in the environment across multiple temporal and spatial scales, require the understanding of that element's speciation (Hesterberg et al., 1999). This concerns the chemical species (isotopic composition, electronic oxidation state, and/or complex or molecular structure) of an element either within the soil matrix or in solution (IUPAC, 2014). The knowledge of element speciation provides the necessary information to understand the behaviour and properties of an element in soils.

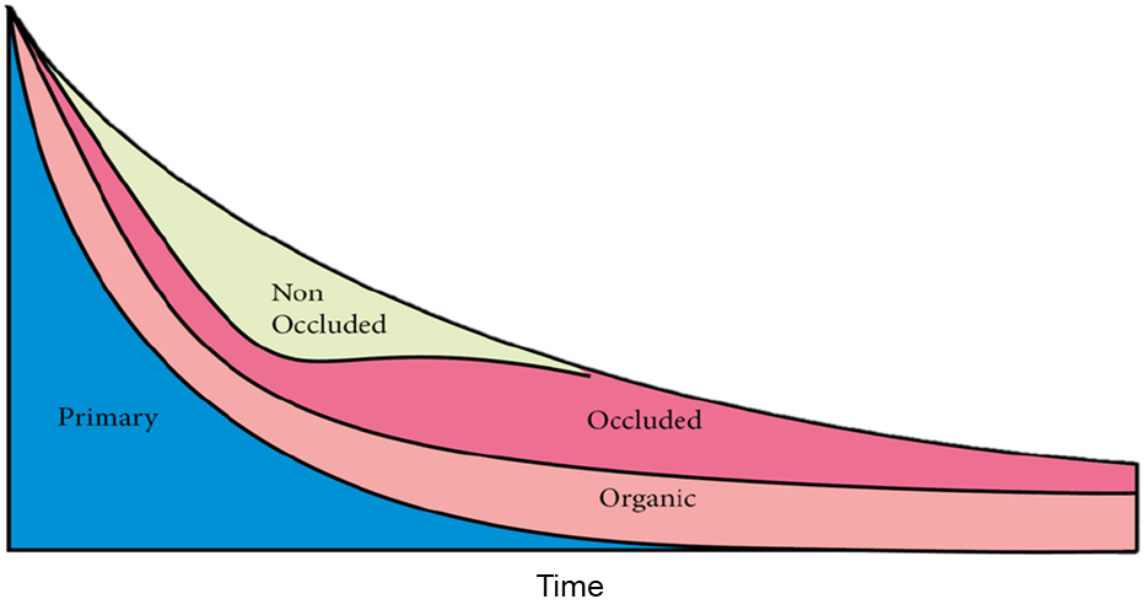

Figure 1. The classic conceptual model of changes in soil phosphorus fractions during pedogenesis (redrawn and modified from Fig. 1 in Walker & Syers (1976)).

In terrestrial ecosystems, the initial source of P is mainly bedrock weathering (essentially apatite rock - $Ca_5(PO_4)_3(OH)$, however in developed ecosystems where the bedrock has been weathered or is poor on P, other input sources like dust deposition and internal cycling are also important (Graham and Duce, 1979; O'Day et al., 2020; Okin et al., 2004). Our

current understanding of the terrestrial P dynamics over pedogenetic time-scales is summarized in Figure 1, which shows that within 12.000 years most of the bedrock P is mobilized As total soil P content decreases over time, clay minerals (e.g. illite, smectites) and other clay-sized minerals (e.g. iron (Fe) and aluminum (Al) -(hydr)oxides) are accumulating in the soil during pedogenesis (Jenny, 1941; Lindsay, 1979). This process creates new surfaces and conditions for the adsorption and/or precipitation of secondary P compounds. Simultaneously organisms are developing on-site, and their turnover contributes to the accumulation of organic P forms in soils. Ultimately, soil development is thought to lead to a "steady-state" in which system P losses equilibrate with system P gains. At this point, only scarce P sources, being inorganic mineral-bound P and/or highly stable organic mineral-bound P compounds, are left to nourish the ecosystem, and the internal cycling of P becomes pivotal for the maintenance of the system (Turner, 2008a; Vincent et al., 2013, 2012).

Along with the evolution of different P forms or species during pedogenesis, the bioavailability of P increases during the early stages of pedogenesis due to the release of orthophosphate to the soil solution from the bedrock and the release of labile organic molecules by plants and microorganisms. As the soil fraction of organic P increases, and microbial processing breaks down complex organic P molecules, the accrual of stable, microbial-derived organic P molecules increases. These small organic P molecules are capable of having strong adsorption bonds to the surfaces of soil minerals (Celi et al., 2000; Wan et al., 2016; Yan et al., 2014). On the other hand, the inorganic P fraction in soils can be also strongly stabilized on surfaces of Al-/Fe-(hydr)oxides, clay minerals, or precipitated with Calcium (Ca) (Gérard, 2016; Lindsay, 1979; Rajan, 1975; Torrent et al., 1992).

At the microscale, different aspects of the P cycle occur simultaneously. For instance, weathering of parent material at the root-soil interface leads to the formation and aggregation of secondary minerals which can retain P with different binding capacity and strength (Garcia Arredondo et al., 2019; Prietzel et al., 2019). These surfaces, being rich in P, can trigger microbial activity where distinct spatial patterns (heterogeneity) will form, depending on the mineralogy of the soils (Adediran et al., 2020; Baumann et al., 2019). These spatial patterns could evolve also according to the P evolution and the equilibrium between the soil-microbiome-plant continuum. Besides mineralogy, the location of secondary minerals within the matrix of soil aggregates affects the spatial distribution of different P species at the aggregate scale (Hesterberg et al., 2017; Werner et al., 2017). Thus, at the microscale, spatial heterogeneity is a product of soil mineralogy and aggregation as drivers, making surfaces

available for preferential adsorption of P. However, the role of distinct P species in the formation of spatial P heterogeneity patterns at present is unknown.

At the macroscale, the stage of the pedogenetic P timeline, in which a given site is, exerts a great deal of control for the distribution of different plants (Turner et al., 2018). In this regard, forests around the world can be found in different stages of the pedogenetic P timeline, independent of forest maturity but rather dependent on the soil P status (Lang et al., 2016). For instance, it is hypothesized that the parts of the Amazon forest located in regions with highly weathered parent material are at a later stage of soil P availability than parts located in regions with less weathered parent material (Fleischer et al., 2019). Meanwhile, Central European forest soils can be found within the initial to middle stages of the pedogenetic P timeline, depending on their initial P budget. In the case of temperate forest soils derived from calcareous parent material, their initial P supply is very low, making forest P nutrition very deficient and fragile to changes. A recent troublesome realization is that Central European forests are losing their ability to efficiently recycle P, probably because of excessive N input and climatic stress (Jonard et al., 2015). Furthermore, forest monitoring data from Central Europe show trends of decreasing P concentrations in tree needles and leaves during the last 20 years with anthropogenic environmental changes being the likely causes (Jonard et al., 2015; Prietzel et al., 2020). Considering that forest P cycling relies mostly on organic P sources as a form of forest internal cycling, it is of pivotal importance to understand both the dynamics of organic P and its association with the turnover of soil organic matter (SOM), *i.e.* soil organic carbon (SOC).

These open questions cannot be answered under the single scope of a scientific discipline, but rather require integrative and interdisciplinary approaches. For this, information from different spatial and temporal scales must be combined to fully understand the nutrition of an ecosystem and to assess the impact of environmental change. Synchrotron-based techniques, like X-ray absorption spectroscopy (XAS) and X-ray fluorescence (XRF) allow the investigation of P and SOM at different scales, by applying either different energies (to probe different elements or different edges of the same element) and/or different modalities of analysis (microbeam and unfocused beam). This thesis applied these different modes of synchrotron-based techniques to investigate the following hypotheses:

a) HS1: In soils with varied P concentration, where self-absorption effects are present, synchrotron-based XANES spectroscopy at the P K-edge is not capable of accurate P speciation

b) HS2: Increasing temperature and its associated vegetation change, does not shift the molecular composition of SOM towards increased decomposition and mineralization of SOC, N, P and S.

c) HS3: Initial soil P speciation does not affect root functional traits and the P and C microspatial distribution at the soil-root interface.

d) HS4: P $L_{2,3}$-edge XANES spectra, which are feature-rich in comparison to P K-edge XANES spectra, do not allow the accurate speciation of different organic and inorganic P compounds.

1.2 Relating P cycling to SOM turnover

The C and P cycles in terrestrial ecosystems are tightly coupled, and it is expected that changes in SOM turnover in temperate forests as consequence of climate warming and global change are also changing the P dynamics. This is because most of the P in forest soils is present in organic forms associated with different SOM fractions. The different inputs of organic P can be (i) aboveground litter fall and subsequent transport into deeper soil layers by bioturbation and water transport, (ii) directly injected into the soil as plant root or plant root exudate, or (iii) microbial acquisition and transformation of inorganic phosphate. Plant inputs are thought to dominate in mature forests, because the speciation of organic P in mature soils often mirrors the molecular architecture of the plant input (Wang et al., 2019).

The molecular variety of organic P compounds is broad (Figure 2), and includes monoester phosphates (e.g. polysaccharides), diester phosphates (e.g. lipids, nucleotides), and phosphonates (e.g. amino phosphonates). The input of most organic P to the soil is in the form of phosphate diesters, which in the course of SOM decomposition are broken down into phosphate monoesters (Wang et al., 2019). Since phosphate monoesters are commonly identified in soils, their stabilization mechanisms in silicate and calcareous soils have been thoroughly investigated. For instance, Phillips et al. (2016) showed that small phosphate monoesters can be enclosed within the calcite structure, while larger compounds like DNA require a larger space leading to longer phosphate-carbonate distances. On the other hand, Al (oxy)hydroxide have shown potential as mediators of inositol phosphate availability due to their high affinity, surface and sorbing energy (Wan et al., 2016; Yan et al., 2014).

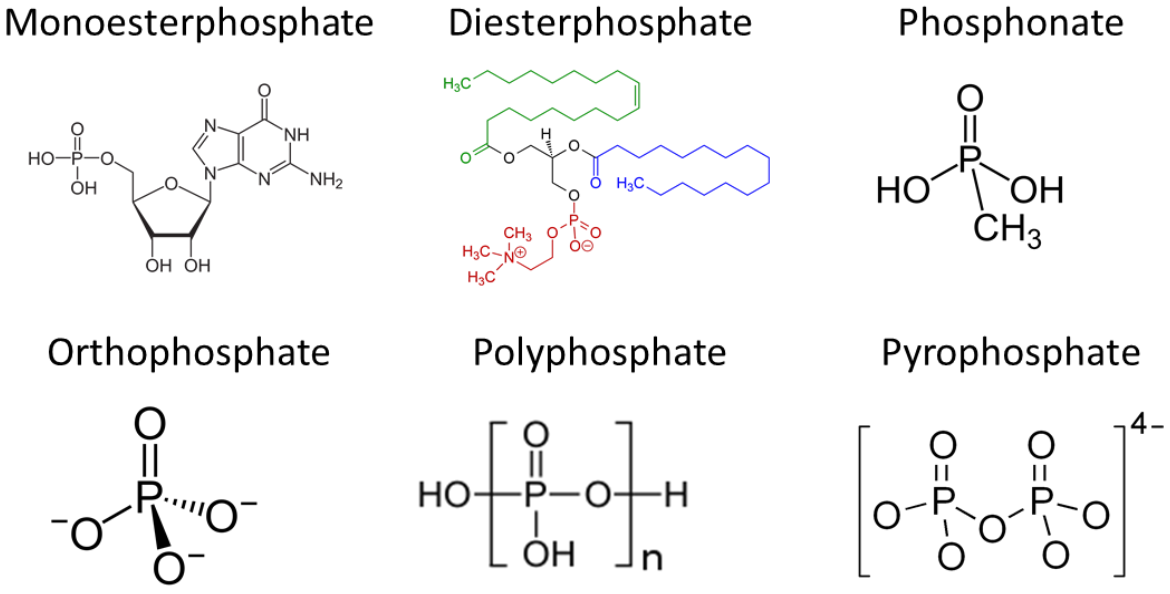

Figure 2. Representative organic (phosphate monoester, phosphate diester, and phosphonate) and inorganic (orthophosphate, polyphosphate, and pyrophosphate) P species.

While the abiotic transformation of organic P in soils is mediated by physicochemical soil properties, the mineralization of organic P is controlled by extracellular enzymes (namely phosphatases). These enzymes cleave the phosphate group from the organic core, making the phosphate bioavailable for plants and microorganisms. The considerable energetic costs of enzyme production limit their exudation by microorganisms and plants alike (Turner, 2008a), and therefore high enzyme activities are mostly found in hotspots within the soil (Zhang et al., 2019). These hotspots are mostly associated with root-soil interfaces (rhizosphere), where root activity shapes these spots and modulates P speciation (Hinsinger, 2001; Werner et al., 2017). Thus, the rhizosphere serves as a micro-spatially constrained reactor for (i) uptake and/or excretion of P in specific forms and (ii) promotion of mineral weathering and pedogenesis (Garcia Arredondo et al., 2019; Hinsinger et al., 2009, 2003). However, at the moment no study has addressed to which extent correlations between spatial heterogeneity patterns of SOM-root systems and spatial patterns of total P, P fractions, or P species in soils are created by biotic (plant+associated microorganism communities) activity. This may include either (i) actively changing the soil P status in intensively rooted soil regions, thus creating soil P heterogeneity, and/or (ii) preferentially rooting soil patches with a particular P status (e.g. zones originally enriched in total P or specific P forms), thus utilizing and exploiting original P heterogeneity.

As illustrated by Figure 2, the organic P forms are often associated with heteroatomic organic moieities (organic molecules containing besides C and H also O, N, S, and/or P). Thus, information of both the P content and species should be integrated into our knowledge of SOM cycling, and vice-versa. Through various spectroscopic techniques, like nuclear magnetic resonance (NMR) and x-ray absorption spectroscopy (XAS), it is possible to both investigate the nature of organic P and of the other major elements that compose SOM (C, N, and S). Nitrogen, for instance, is a major component of proteins and amino sugars, but also of heterocyclic compounds like DNA; on the other hand, S has both a major function as protein co-factor and through its oxidation can also aid in the acquisition of adsorbed P by microorganisms.

This holistic understanding of SOM cycling is only possible through the correct application of these novel spectroscopic techniques, and the investigation of new modes of analysis, like cryo-microspectroscopy.

1.3 Approaches for the analysis of P at the macro and microscale

1.3.1 Liquid state ^{31}P NMR spectroscopy

Nuclear Magnetic Resonance (NMR) spectroscopy is a powerful and versatile technique to probe the molecular structure of soil components like SOM but also soil minerals (Mao et al., 2017; Wilson, 1987). The most common application of NMR spectroscopy in soils is the use of ^{13}C NMR through solid-state NMR techniques such as cross-polarization magic angle spinning (CP-MAS) NMR (Courtier-Murias et al., 2014; Kögel-Knabner, 2000). Furthermore, it is the standard technique for P speciation, though liquid state ^{31}P NMR spectroscopy (Cade-Menun and Liu, 2013; Turner, 2008b). The advantage of ^{31}P NMR is that contrary to other elements like C, phosphorus consists of only one stable isotope, ^{31}P, which is NMR-visible with high sensitivity. However, while all P in a soil sample are visible for NMR, the low concentration of P in soils complicates its analysis in solid-state (Vincent et al., 2012). Thus, P extraction and analysis in a liquid state is currently the best workflow for ^{31}P NMR spectroscopy of soils (Turner et al., 2005). As a result, liquid state ^{31}P NMR spectroscopy has allowed the identification, structure elucidation, and quantification of a wide variety of P-containing molecules in soils (Cade-Menun, 2015).

NMR conducted on liquid samples requires that the P in the soil specimen is extracted into the solution to be used for the NMR experiment. Several extraction procedures have been developed, using strong bases or acids or sequential fractionation schemes. However, the current gold-standard is a single-step extraction using sodium hydroxide/ethylenediamine tetraacetic acid (NaOH/EDTA) treatment developed by Cade-Menun and Preston (1996). A typical 1D ^{31}P NMR spectrum of the Of layer of an alpine temperate forest soil is shown in Figure 3. In this spectrum, many peaks are visible, with different positions on the frequency x-axis (expressed as "chemical shift" with ppm as unit). In theory, each signal can be related to an individual P species based on its specific chemical shift value, which depends on the specific molecule and the conditions in the solution. Thus, initial research focused on producing information on the spectra of single components and extracts from model mixtures and natural soils, intending to unambiguously identify P compounds in NaOH/EDTA extracts. The published chemical shift regions defined the assignments of different P species in Figure 3.

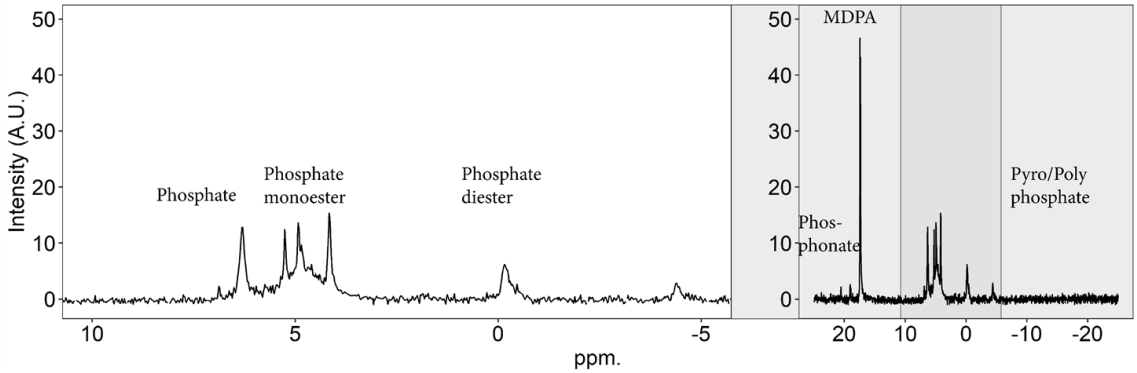

Figure 3. Liquid state ^{31}P NMR spectrum of the Of layer of an alpine temperate forest soil, spiked with methylene diphosphonic acid (MDPA), as internal standard.

Here we can observe that most soil organic P is composed of phosphate mono- and diesters. Furthermore, the spectrum also reveals less abundant P species such as phosphonates and inorganic phosphate compounds. The grouping displayed in Figure 3 allows for a basic interpretation of the total P composition; however, for a mechanistic understanding of the P cycle, the identification/quantification of individual species is necessary. In liquid-state ^{31}P NMR spectroscopy, the difficulty lies in the correct identification and quantification of coexisting several types of phosphate mono- and diesters. This is because, while the chelating power of the EDTA presumably extracts all bio-available P, the extraction also alters the chemical structure of various P species (hydrolysis of diesters), while also adding paramagnetic elements to the solution (e.g. Fe^{3+}, Mn^{2+}) (Doolette et al., 2011; Smernik et al., 2015). This leads to signal broadening and chemical shift dispersion of the ^{31}P nuclei in these compounds.

Soil scientists tackled this problem by doing spiking experiments to help identifying the main components of the organic P fraction. However, different species of the same P family, such as several monoesters can have the same chemical shift, and/or can be degradation products of another P family. A novel approach for the correct identification of organic P compounds based on NMR was developed by Vestergren et al., (2012). They applied a 2D NMR technique called heteronuclear single quantum coherence (HSQC), which allows the unambiguous identification of many P signals according to chemical shift information from two (^{1}H and ^{31}P) domains and characteristic J-coupling interactions between P-C-H or P-O-C-H chemical bonds. The result is a 2D plot, where based on the chemical shift from protons correlated with P from different molecules, a cross peak in the 2D plot will be visible and allows the differentiation of molecules even within the same group. This technique has brought light to the shifts in P composition in both boreal and temperate forests (Vincent et al., 2013, 2012; Wang et al., 2019).

Despite improvements in spectral resolution with the application of the HSQC technique, some shortcomings of ^{31}P NMR, like the misidentification of some compounds and the low extraction efficiency continue to exist (Doolette et al., 2010; Smernik and Dougherty, 2007; Smernik et al., 2015). Furthermore, spatial information at the micro- or nanoscale is unattainable with NMR. For this reason, an increasing interest exists in methods that can probe the total P of soils and quantify different P species in a spatially resolved manner. Among many physical methods, synchrotron-based methods have gained notoriety and have the potential to change our concepts of P dynamics in soils, like they have done for C (Lehmann et al., 2008).

1.3.2 Synchrotron-based methods

Synchrotron storage rings, in their most pure sense, are – simply put – very powerful sources of electromagnetic radiation in the X-ray regime (synchrotron light). They provide light by circulating high-energy electrons through a storage ring. These electrons emit synchrotron light at the tangent of their orbital path at positions defined by multi-layered magnets (known as bending magnets and insertion devices). This light can be directed into hutches for a wide variety of applications, as a beam focused, tuned from the far-infrared to the hard x-ray regime with high 'brilliance'[1] (Willmott, 2019). Different types of interaction between light and matter provide insight and information about the sample at an unprecedented level of detail. Thus, synchrotrons are the to-go facility when investigating complex surfaces, materials, and processes. Soils, as the most complex natural-engineered material, are not an exception, and the investigation of soil surfaces and processes has greatly benefited from synchrotron facilities in the last decades (Fendorf et al., 1994).

A common application of synchrotron light is to analyze the shifts in the absorption coefficient (μ) of an element of interest as a function of the incident X-ray energy; this is commonly referred to as X-ray Absorption Spectroscopy (XAS)(Hesterberg, 2010). In essence, absorption events occur when a photon incident on a sample interacts with sample electrons and releases all its energy, disappearing in the process. The photons, prior to their disappearance, cause transitions of the target sample electrons from lower atomic energy levels to higher levels, leaving a vacancy in the low energy levels. The vacancy in the low energy levels is filled by the transference of high energy electrons to low energy levels. By doing so, electrons may release energy radiatively as a fluorescent photon with lower energy than the incident energy of the primary X-ray photon or non-radiatively by expelling a so-called "auger

[1] Brilliance: a figure of merit of synchrotron facilities defined as: $\frac{number\ of\ photons}{second * source\ area\ (mm^2) * source\ angular\ divergence\ (mrad^2)}$

electron". These excitations are monitored as shifts in the X-ray absorption coefficient (μ), which is related to the absorption cross-section per mass basis, and express the strength or probability of an interaction between the incident X-ray photons and the electrons of the element of interest per amount of the element. Absorption events occur by photon-electron interactions at a specific energy which binds electrons to its shell, and which is unique for different elements and electron orbitals. A typical XAS spectrum at the P K-edge of hydroxyapatite is shown in Figure 4.

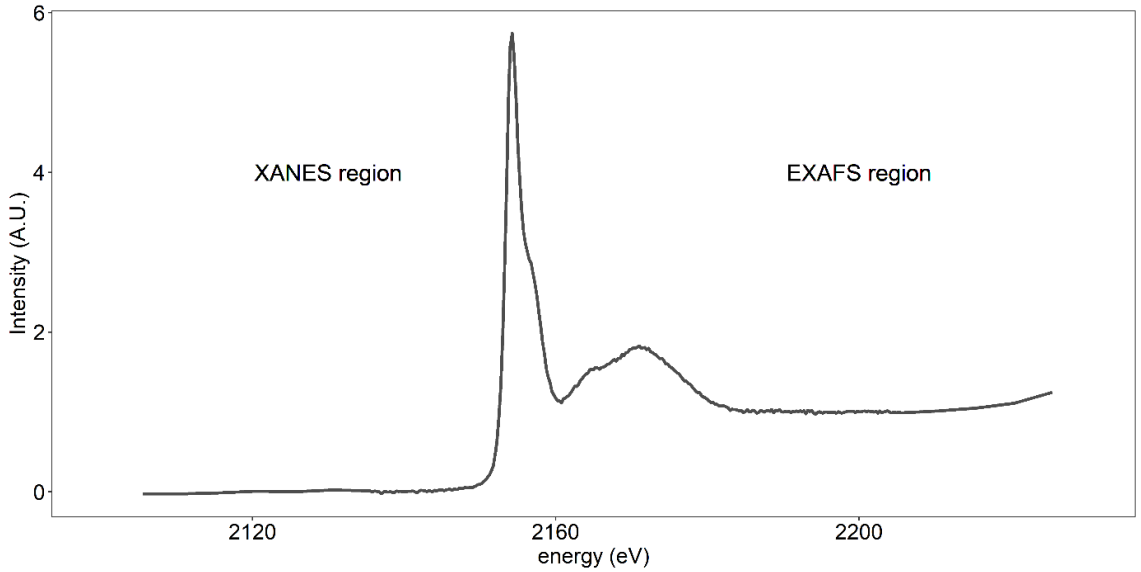

Figure 4. P K-edge XANES spectrum of hydroxyapatite with the XANES and EXAFS regions.

The XAS spectrum (s. Figure 4) consists of a sequence of structures (features or peaks) having a characteristic intensity, width, and energy (eV). The spectrum can be divided in two regions, the "near-the edge" and the "extended edge", formally known as the X-ray Absorption Near Edge Fine Structure (XANES) and the Extended X-ray Absorption Fine Structure (EXAFS), respectively. There is a disparity in the current level of theoretical understanding of the XANES region and the EXAFS region. The EXAFS region can be summarized as the average signal given by the photo-electrons radiating in all directions from our element of interest and having constructive or destructive interferences with itself after the interaction with neighbouring atoms, under single scattering events (Bunker, 2010). The deeper level of understanding of the EXAFS region, reflected in the EXAFS equation (eq. 1), with allows the possibility of extracting, for instance, the interatomic distance between atoms of the material of interest (Rehr et al., 1998).

Eq. 1[2] $$\chi(\mathrm{k}) = \sum_j \frac{N_j f_j(k) e^{-2k^2\sigma_j^2}}{kR_j^2} \sin[kR_j^2 + \delta_j(k)]^2$$

Meanwhile, the XANES region, that reflects multiple scattering events, which are harder to theoretically represent and to extract meaningful information from (Mottana, 2004). Yet, since this region encompasses the strongest intensity and width changes in the spectrum, it can be used to fingerprint known compounds in an unknown standard. This allows the identification and (semi-) quantification of different species of the element of interest in the sample. Two common approaches are (1) the use of known standards to fit a model via least-squares fitting the spectrum sample (linear combination fitting – LCF), and (2) the use of theoretical Gaussian functions to represent different species of the investigated element in the spectrum (Gaussian fitting). The case of P, a low Z element, with low concentration in soils and with an absorption edge of its core-shell within the intermediate (hereafter named "tender") X-ray energy range, means that the absorption of this element is mostly monitored through the fluorescence (XRF) event sparked by the absorption.

While the measurement of the K-edge XANES is currently the standard approach for P speciation using XANES spectroscopy, this approach has some caveats (Hesterberg, 2010). For instance, the K-edge is not a valence shell for P, which means that the transition probed is 1s → 3p. This fact affects the spectral features due to the poor energy resolution at the metal K-edge caused by the short lifetime of the 1s core hole. On the other hand, a valence shell like the $L_{3,2}$-edge, which is related to the transition from $2p_{3/2}$ to $2p_{1/2}$ orbitals, has a longer lifetime hole, which translates into a higher energy resolution of its spectral features (Kruse et al., 2009). While the L-edge of phosphorus is not its valence shell, its distance from the nucleus makes it more sensitive to the different chemical environments where phosphate can be found in soils. This in essence means that the spectrum of the P K-edge has only subtle features and does not allow the precise identification of compounds from the same group. In contrast, the spectrum of its $L_{3,2}$-edge is richer in features and thus has the potential to identify a greater variety of P compounds; yet its potential is currently unexplored (Kruse et al., 2015).

Another potential inconvenience of the current approach for the P K-edge XANES is that measurements are susceptible to distortions due to self-absorption effects. Self-absorption is the systematic, energy-dependent reduction in the experimentally measured fluorescence

[2] $f_j(k)$: Effective scattering amplitude
N_j: Coordination number
$\delta_j(k)$: Phase shift
$e^{-2k^2\sigma_j^2}$: Amplitude damping terms due to electron escape depth
R_j: Interatomic distance

amplitude (Rehr and Albers, 2000). Previous approaches to correct self-absorption are based on mathematical algorithms aiming to correct the fluorescence yield distortions (Trevorah et al., 2019). Yet, most of these approaches rely on knowledge of sample stoichiometry, measurements of multiple angles, or exact knowledge of the energy dependence of the absorption coefficients (Booth and Bridges, 2005; Goulon et al., 1982; Trevorah et al., 2019; Tröger et al., 1992; Trevorah et al., 2019). These conditions are hard to meet in environmental samples. Thus it is recommended to avoid self-absorption effects rather than attempting to correct them (Kelly et al., 2008).

With these caveats in mind, synchrotron-based XANES spectroscopy has still the advantage of being able to probe in-situ the spatial P distribution at the micro-scale. This can be done through spatially -resolved synchrotron-based X-Ray fluorescence (μ-XRF), which allows to map the spatial distribution of several elements at the same time. This technique has the potential to unlock at the same time the spatial distribution of P, together with other important elements in the soil matrix (e.g. Fe, Al, Ca, and C). Additionally, μ-XRF measurements can be energetically resolved at points of interest (μ-XANES) or as energy stacked maps of μ-XRF, similar to common scanning transmission x-ray microscopes (STXMs), thus allowing the elucidation of the microspation distribution patterns of different P species in addition to total P concentrations. So far, only very few studies have investigated P at the microscale (Adediran et al., 2020; van Veelen et al., 2019; Werner et al., 2017), and when done, in most cases fixing agents like resins have been used to maintain the structural integrity of the sample. However, the use of resins for soil microanalysis may cause artificial changes in sample chemistry and/or structure (Refshauge et al., 2006). More importantly, if our interest is to study C-P interactions, adding a C-rich resin to the sample prevents the mapping and, if desired, speciation of C through synchrotron methods. However, just as resin also cryo-fixation also maintains the structural integrity of soil samples without adding undesired C. Furthermore, using cryo-fixing methods has the potential to minimize radiation damage effects on the sample (Leontowich et al., 2016). The use of μ-XRF and μ-XANES has the potential to unravel the micro-spatial distribution of P within model systems and point us towards critical changes o P speciation mediated by biotic and abiotic factors.

1.4 Objectives and Approach

The overarching research aim of this thesis is to integrate and apply current knowledge of P speciation techniques in order to understand the spatial heterogeneity and shifts of P species in soils at macro (plot scale) and microscale (root-soil interface). To achieve this aim, the following objectives were constituted:

(1) What is the optimal concentration of P to collect data in X-ray fluorescence mode, at which spectra and consequently LC fitting results are not significantly influenced by self-absorption?

(2) How do recent improvements in data processing optimization affect LC fitting results of P XANES spectra even when self-absorption is present?

(3) What steps are necessary to use P -$L_{2,3}$-edge XANES spectroscopy for the speciation of organic and inorganic P species in soils?

(4) To what extent can P-$L_{2,3}$-edge XANES spectroscopy detect changes in organic and inorganic P species?

(5) How do temperature and its associated vegetation changes modulate the speciation of P, C, N, and S in temperate mountain forest soils?

(6) How can synchrotron-based speciation data obtained on different elements be integrated to understand the deeper effects of temperature on SOM chemistry?

(7) How does initial soil P speciation affect root functional traits (diameter, specific surface area, length) and the acquisition mechanisms by plants?

(8) How do different root functional traits affect the microspatial distribution of C and P in soils, and what is its relation to the key P acquisition mechanisms by plants?

These objectives were approached through three main projects:

Project 1: Improvement of analytical synchrotron-based X-ray spectroscopy methods for the analysis of phosphorus in soils (Objectives 1, 2, 3, 4). The speciation of phosphorus in soils is critical to understand its turnover and dynamics in terrestrial ecosystems. Therefore, one important goal of this thesis was to optimize current synchrotron-based P K-and $L_{2,3}$-edge

XANES spectroscopy methods in order to achieve a most correct (i.e. precise and accurate) quantification of different organic and inorganic P species in soils.

Project 2: Investigation of concomitant C, N, P, and S speciation changes in mountain forest soils across a temperature gradient (Objectives 5, 6). Aware of the great power of combined XANES and NMR spectroscopy for the analysis and speciation of carbon (C), nitrogen (N), P, and sulphur (S) in soils, I investigated the influence of a temperature gradient on the C, N, S and P speciation in a mountain forest soil toposequence with a synoptic approach. Additionally, I combined these chemistry-focussed studies with microbiological analyses (soil microbial bio- and necromass, community composition, enzymatic activity).

Project 3: Evaluating the influence of soil phosphorus speciation and soil mineral composition on the root functionality of *Picea abies* L. seedlings and associated microspatial distribution patterns of C and P in silicate and calcareous soils (Objectives 7, 8). Motivated by the observation of organic P accumulation in temperate forest soils, I aimed to understand the processes responsible for the organic P accrual. I produced artificial soils with contrasting initial soil P speciation (organic *vs.* inorganic P) and mineral composition (silicate- *vs.* dolomite-based), and cultivated *Picea abies* L. seedlings on microcosms containing the different soil variants in a two-factorial experiment with respect to soil P form and mineral composition.

The three projects were executed in four studies, each represented by a publication a in peer-reviewed journal

In *Studies 1a and 1b*, both assigned to **Project 1**, I developed two novel approaches for soil P analysis using XANES spectroscopy. *Study 1a* reveals the shortcomings of P K-edge XANES in soil samples with high P concentrations and highlights the use of new computational tools to minimize analytical errors for such soils. *Study 1b* presents a novel method for the analysis of P $L_{2,3}$-edge XANES spectra, which allows a better quantification of organic P species in soils and other environmental materials.

The findings of *Study 2,* assigned to **Project 2,** revealed the synergetic changes of SOC, N, S and P stocks and speciation in forest soils across a temperature gradient. At a lower temperature (forest dominated soils), the SOC was mostly lignin-associated, the N was mostly protein-associated, and the P was mostly organically bound, while at a higher temperature (alpine meadow-dominated soil), SOC-lignin, N-protein and organic P were largely decomposed, associated with an accrual of SOC-lipids, heterocyclic N, and inorganic P. These

processes could not have been identified by any single soil analysis, but only by their combination. Thus, my combined approach has been shown to be of fundamental importance for the analysis of abiotic disturbance impacts on C and nutrient cycling in temperate forest ecosystems.

The findings of *Study 3* assigned to **Project 3**, revealed that the initial soil P speciation modulates functional root traits expressed by plants, inducing different C, N and P dynamics in soils. Roots of *Picea abies* L. seedlings grown in inorganic P-rich soils were thinner and longer than roots of *Picea abies* L. seedlings grown in soils that were rich in organic P, but otherwise identical. This led to a higher SOC accumulation in the soils with inorganic P compared to those with organic P amendment. However, at the microscale, in the soil with organic P amendment soil regions with particular P enrichment were also zones with particular enrichment of organic C. Thus, fine-scale microspatial analysis suggests that root-microbial association and cooperation may be a more important mechanism for the acquisition of organic P than for inorganic P by plants, independent of soil mineralogy. Here we demonstrate the importance of microscale spatial distribution to reveal key processes of plant P acquisition from soils.

2. Materials and Methods

2.1 Study sites and sampling

2.1.1 Soils with high natural P content (Studies 1a and 1b)

The different soils used for each study reflect the inherent needs of each work to analyze P species under specific conditions. While *Study 1a* focused on the effects of self-absorption on spectral interpretation, *Study 1b* focused on the speciation of organic P, thus requiring the investigation of a soil with high organic P content. For *Study 1a,* I used a soil sample from the district of Lapão, State of Bahia, Northeast region of Brazil (UTM 187881 and 8736316, zone 24S), inside the Irecê Plateau. The soil is an Inceptisol (Soil Survey Staff, 1999). From this soil, I chose a subsurface layer (90–140 cm deep) with 28.26 g P kg^{-1}. On the other hand, in *Study 1b* I analyzed two P-rich soils from a penguin colony site located on Deception Island (South Shetland Islands, Maritime Antarctica). Soil samples were taken on a site with an active moss layer (5.32 g P kg^{-1}) and on another site with a dead moss layer (3.92 g P kg^{-1}).

2.1.2 Temperature gradient in the German Alps (Study 2)

I combined two temperature gradient sets located in different mountain ranges (Mangfall and Karwendel) in the German Limestone Alps (Figure 5). Site *Langenau* (LAP) is located in the Mangfall Mountains, and comprises four plots: (i) LAP-N, (ii) LAP-S, (iii) LAP-D, and (iv) LAP-Z. Site *Seinsberg* (SEI) is located in the Karwendel Mts. and comprises three plots: (i) SEI-Z, (ii) SEI-D, and iii) SEI-A. A detailed description of the sites is provided in Prietzel and Ammer (2008).

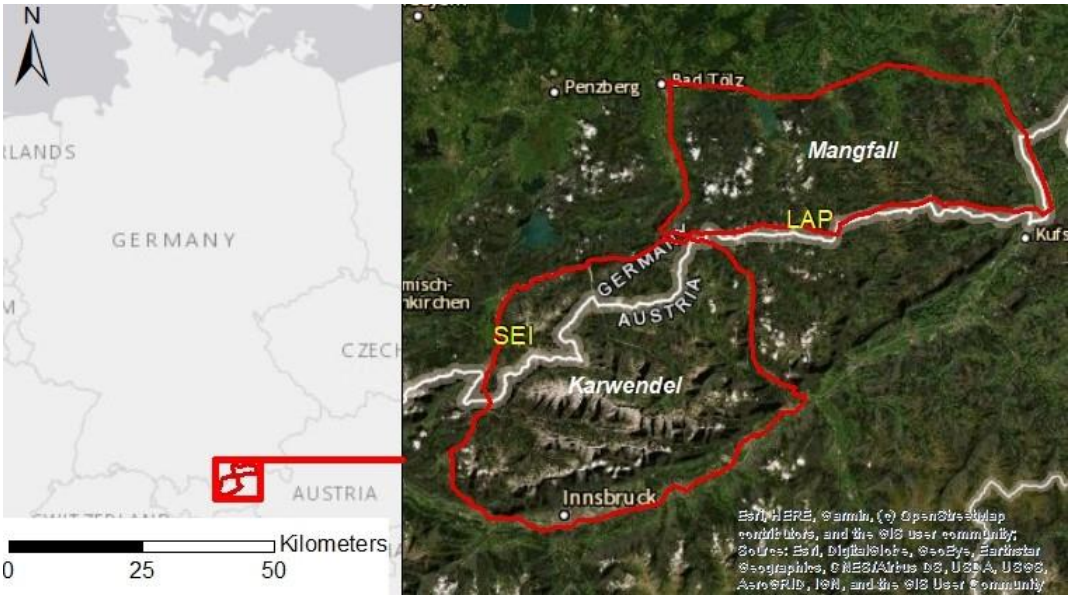

Figure 5. Location of sites Seinsberg (SEI) and Langenau (LAP) in the Karwendel and Mangfall mountain ranges.

I monitored climatic variables by positioning Tiny tag® data loggers (Gemini Corp. Chichester, UK) to record air temperature and relative humidity 1 m above ground level, and soil surface temperature as well as subsurface temperature (5 cm below soil surface) in hourly intervals between May 2017 and April 2018. Thereafter, I calculated the mean weekly and annual values for each climatic variable. Soil sampling was done in five soil pits for undisturbed samples, which were randomly distributed over the respective plots. A detailed site description is provided in Table 1.

From each horizon of every soil pit, undisturbed samples of the mineral soil (Ah) and organic horizons (Of, Oh), if present, were collected for chemical analyses. Additionally, for biochemical analyses, I sampled disturbed samples of the mineral soil and organic horizons at three soil pits at every site. To guarantee comparability of the soil biology, all disturbed samples were taken close to *Acer pseudoplatanus* L. trees, if present, associated with arbuscular endomycorrhiza, as well as *Fagus sylvatica* L. and *Picea abies* L. trees, both associated with ectomycorrhiza. Soil samples were transported in cooling boxes, followed by storage at -20°C in the lab. Field-moist subsamples for biological analyses were sieved to <2mm and stored at –20°C, and thawed only immediately before analysis. For chemical analyses, I dried subsamples at 60°C to constant weight, removed roots and coarse woody debris, and sieved the soil to < 2 mm. A subsample of the sieved soil material was ground in a ball mill to a particle size of <100 μm.

Table 1. Basic site description for the Karwendel (SEI) and Mangfall (LAP) sites.

Mountain range	Site	Latitude, longitude	Air MAT (°C)	Relative humidity (MRH%)	Soil surface MAT (°C)	Soil subsurface MAT (°C)	Vegetation
Mangfall	LAP-N	N47° 36.132, E11° 49.165	6.8	82.6	7.8	7.6	P.a., A.a., F.s., A.p.
	LAP-S	N47° 36.328, E11° 48.497	7.3	76.2	8.1	7.7	P.a., A.a., F.s., A.p.
	LAP-Z	N47° 36.341, E11° 48.408	7.3	81.4	8.2	7.9	P.a., A.a., F.s., A.p.
	LAP-D	N47° 36.324, E11° 48.408	7.7	80.5	9.6	9.2	P.a., A.a., F.s., A.p.
Karwendel	SEI-Z	N47° 28.337, E11° 18.434	6.5	82.2	7.0	6.9	P.a., A.a., F.s., A.p.
	SEI-D	N47° 28.350, E11° 18.327	6.8	80.6	7.8	7.6	P.a., A.a., F.s., A.p.
	SEI-A	N47° 28.348, E11° 18.339	7.0	76.2	10.1	10.0	C.

P.a.: *Picea abies* L., A.a.: *Abies alba* Mill., F.s.: *Fagus sylvatica* L., A.p.: *Acer pseudoplatanus* L., C.: *Calamagrostis spp* Adans.

2.2 Microcosms experimental design (Study 3)

I produced two different artificial soils of well-defined composition to act as models for soils derived from either silicate or calcareous bedrock. For each soil variant, I prepared 50 g of ferrihydrite (FH) synthesized according to Schwertmann and Cornell (1993), and 50 g of Al-saturated montmorillonite (Al-MT) according to Bouazza et al. (2006), and 50 g of a 1:1 (w/w) mixture of FH and Al-MT. These minerals were separately loaded with an inorganic P solution (NaH_2PO_4) at pH 5 as described by Prietzel et al. (2016); in the case of the calcareous variant, hydroxyapatite (HydAp) substituted the P-loaded FH as inorganic P source. Another set of

the same minerals was loaded with organic P (inositol phosphate – IHP); here calcite loaded with organic P substituted the FH variant loaded with organic P. The pure and mixed phases of P-loaded FH, Al-MT, and HydAp were diluted and homogenized with silt-sized quartz (silicate soils) or dolomite (calcareous soils) and sand-sized quartz to a final P content of 0.5 g kg^{-1}, yielding 1.000 g of each variant.

Each of the four soil variants was distributed in small pots, together with a diluted solution of organic layer from either a silicate soil (Dystric Cambisol *Mitterfels*; Prietzel, 2020) or calcareous soil (Rendzic Leptosol *Guggenauer Köpfl*; Prietzel, 2020)to inoculate the artificial soils with the natural microbial communities of these soils. In five pots (microcosms) of each the four soil type (silicate, calcareous)/P addition (inorganic P, organic P) combination variants, 40 seeds/pot of Norway spruce (*Picea abies* L.) were applied, five pots of each soil type/P addition combination variant remained unseeded so serve as control variants. Thereafter, the microcosms were incubated in a growth chamber at constant temperature (25°C), sunlight intensity (50%), and light duration (12 hrs). After germination, six seedlings were left in each microcosm, and the remaining seedlings were removed with tweezers. The seedlings and the control variants were irrigated with a diluted nutrient solution at regular intervals and incubated for 3 months (Figure 6).

During harvesting, shoot and root biomass of the *Picea abies* L. seedlings were separated, shoots were frozen in liquid nitrogen while roots were stored for subsequent analysis. A great portion of the soils was occupied by the spruce roots; therefore I assumed that the entire soil solution within the microcosm was influenced by the roots or so-called rhizospheric soil. After harvesting, the soils were air-dried, sieved to fine earth (< 2mm), and stored until further analysis.

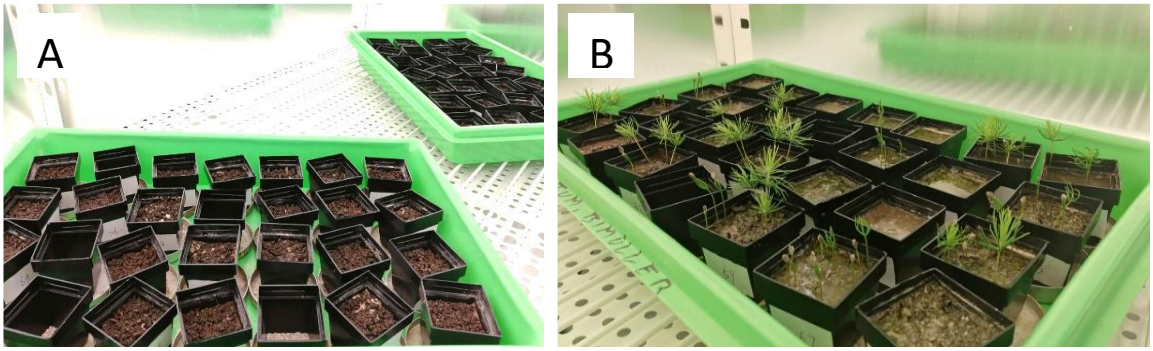

Figure 6. Norway spruce (Picea abies L.) *incubation stages with (A) the first day, (B) two months.*

2.3 Standard compounds and standard physical mixtures

I analysed several standards and standard physical mixtures for my studies. In *Study 1*, I produced a mixture of 33% (P mass) calcium hydrogen phosphate (CAS Number: 7757-93-9), 33% aluminum phosphate (CAS Number: 7784-30-7), and 33% iron(III) phosphate (CAS Number: 13463-10-0), with a final P concentration of 6487.56 mmol kg^{-1}. The standard mixture was finely ground and then diluted in boron nitride (CAS Number: 10043-11-5) using a Wig-L-Bug® grinder/mixer to achieve the following final P concentrations: 1, 6.25, 12.5, 25, 50, 75, 100, 200, 300, 400 and 1000 mmol P kg^{-1}. Meanwhile in *Study 1b*, I diluted each reference standard with fine-ground (mesh 230), high-purity quartz "purum" (Sigma−Aldrich, CAS No. 14808-60-7) to a final concentration of 40 g P kg^{-1}, using an agate mortar and pestle. The used standards for each study are described in detail in Table 2.

In *Study 1b,* I produced three sets of defined artificial ternary and quaternary mixtures by weighing different amounts of the seven diluted reference standards in various combinations to 1 g of sample, and homogenizing them manually with agate mortar and pestle. Set A contained three organic P compounds and one inorganic P form (Set A: inorganic P as hydroxyapatite, P monoesters as phytic acid, P diesters as DNA sodium salt, and phosphonates as methyl phosphonic acid). Set B contained three inorganic P compounds and one organic P form (hydroxyapatite, iron(III) phosphate, aluminum phosphate, and phytic acid as an organic phosphate), and Set C four organic P compounds (P monoesters as phytic acid, P diesters as DNA sodium salt, phosphonates as methyl phosphonic acid, and adenosine 5'- triphosphate as polyphosphate). I proceeded in this way to validate the robustness of the P $L_{2,3}$-edge XANES spectrum deconvolution method for a broad range of P species proportions. In total, 40 diluted ternary and quaternary mixtures of the standards were produced.

Table 2. Reference Compounds used in Studies 1a and 1b.

Compound	Group
Inorganic P form	
Iron(III) phosphate	Iron phosphate
Hydroxyapatite	Calcium phosphate
Calcium hydrogen phosphate	Calcium phosphate
Tribasic calcium phosphate (TCP)	Calcium phosphate
Aluminum phosphate	Aluminum phosphate

	Organic P form
Phytic acid sodium salt hydrate	Monoester phosphate
Deoxyribonucleic acid sodium salt	Diester phosphate
Methyl phosphonic acid	Phosphonate

2.4 Chemical analyses

On the fine-ground soil samples (*Studies 2 and 3*), soil total carbon, nitrogen, and sulfur contents were measured by dry combustion (CHNSO Elemental Analyzer, Hekatech, Wegberg – Germany). The inorganic C (IC) was measured using a Calcimeter (Eijkelkamp, Giesbeek) and a tested Scheibler method (Prietzel and Christophel, 2014), and thereafter the OC content was obtained by subtracting the IC from the soil total C. Total P was measured by digestion of fine-ground subsamples with a mixture of concentrated $HClO_4/HNO_3/HF$ (Chang and Jackson, 1958) and subsequent analysis of the digests by ICP-OES (Varian Vista-Pro CCD). Organic P was analyzed according to Saunders and Williams (1955).

2.5 Microbiological analyses

2.5.1 Total microbial biomass, and fungal and bacterial communities' biomass

Total microbial biomass in all samples of *Study 2* was estimated by the chloroform fumigation extraction method. Briefly, 10 g of fresh soil was fumigated with chloroform, followed by extraction with potassium sulfate (K_2SO_4). Thereafter, concentrations of total organic carbon (TOC) and total nitrogen (TN) were analyzed (Brookes et al., 1984). We corrected for the remaining C using the extraction factor kEC (Joergensen, 1996) for microbial carbon.

Meanwhile, fungal and bacterial communities biomasses were estimated by extracting the phospholipid and neutral lipid fatty acids, using the PLFA and NLFA method described by Bligh & Dyer (1959), with modifications as described by White et al., (1979) and Bardgett et al., (1996). We extracted the lipids from 1 g moist mineral soil, or 0.5 g moist organic layer, with a chloroform-methanol solution. Depending on the respective soil water content we added adjusted volumes of 0.15 M citrate buffer (Bligh and Dyer, 1959). After extraction for 2 h on a horizontal shaker and an additional volume of Bligh and Dyer solution, the samples were centrifuged for 10 min at 2500 rpm. The lipids in the supernatant were isolated by phase separation with chloroform and citrate buffer. The NLFAs were separated via solid-phase extraction in silica columns using chloroform, while the PLFAs were eluted using methanol. Both PLFAs, NLFAs, and the internal standard (C19:0) were methylated under mild alkaline conditions (Dowling et al., 1986), dissolved in isooctane, and analyzed chromatographically with a GC-FID. For each sample, the abundance of fatty acid methyl esters was expressed per unit dry weight. Fatty acid nomenclature was used as described by Frostegård et al. (1993). Gram-positive bacterial biomass was quantified using the fatty acids i15:0, a15:0, i16:0, and i17:0. Gram-negative bacterial biomass was quantified using the fatty acids cy17:0 and cy19:0. For total bacterial PLFAs, the sum of gram-positive and gram-negative bacterial fatty acids as well as of the fatty acid 16:1ω7, were used (Frostegård et al., 1993). For fungal biomass (accounting for saprotrophic fungi and ectomycorrhizal biomass) the fatty acids 18:2ω6 was used (Federle et al., 1986). Meanwhile, arbuscular mycorrhiza was quantified by the NLFA 16:1ω5c (Hedlund, 2002; Ngosong et al., 2012; Ruess and Chamberlain, 2010).

2.5.2 Fungal and Bacterial necromass

We estimated the necromass C by extracting the soil amino sugars (muramic acid, glucosamine, mannosamine, galactosamine), as described by Zhang and Amelung (1996) and Liang et al.

(2012). Briefly, finely ground 400 mg of soil was hydrolyzed with 10 mL of 6 M HCl solution at 105°C for 8h. The hydrolysate was filtered, and the filtrate was completely dried in a rotary evaporator at 40 ºC under vacuum. The residue was purified through neutralization with 0.4 M KOH solution and precipitation of salts in methanol and deionized water. The samples were derivatized to aldonitrile acetates using 32 mg ml^{-1} hydroxylamine hydrochloride and 40 mg ml^{-1} 4-(dimethylamino) pyridine in pyridine-methanol (4:1, v/v) solution. The dried extracts were then dissolved in ethyl acetate plus hexane solution (1:1, v:v) and analyzed via GC-FID (Angst et al., 2018). We quantified the amino sugars using calibration curves derived from an external standard based on different concentrations of target analytes. Contents of muramic acid and glucosamine were used to estimate bacterial and fungal necromass C according to Liang et al. (2019).

2.5.3 Potential enzyme activities

We measured the potential activity of phenol oxidase (EC 1.10.3.1), β-glucosidase (EC 3.2.1.21), leucine-aminopeptidase (EC 3.4.11.1), acid phosphomonoesterase (EC 3.1.3.2), and phosphodiesterase (EC 3.1.4.17). Phenol oxidase was measured using 2,2-Azino-bis-(3-ethylbenzothiazoline-6-sulfonic acid (ABTS) as a substrate (Floch et al., 2007; Koleva et al., 2002). For this, 0.4 g of field-moist soil was suspended in water (1:125, w/v) and dispersed using low-energy sonication (50 J s^{-1}) (Stemmer et al., 1998). Thereafter, 100 µl of soil suspension, 100 µl of buffer (modified universal buffer, pH 3), and 50 µl of ABTS were added into a 96 well plate, which was incubated at 30 °C. Absorption measurements (λ=414 nm) were then performed every 3 min. The enzymes ß-glucosidase, leucine-aminopeptidase, and both phosphatases were investigated with a fluorimetric microplate assay (Marx et al., 2001). The ß-glucosidase activity was determined with MUF-D-glucoside, leucine-aminopeptidase activity with L-leucine-AMC, and both phosphatase activities with MUF-phosphate. For this, 1 g of field-moist soil were suspended in water (1:50, w/v) and dispersed through sonication. Thereafter, 50 µl of soil suspension, 50 µl of buffer (0.1 M-(N -morpholino) ethanesulfonic acid buffer (pH 6.1) for MUB substrate, or 0.05 M TRIZMA buffer (pH 7.8) for AMC substrate), and 100 µl of substrate were added into a 96 well plate, which was incubated at 30 °C. Fluorescence measurements (λ=460 nm) were then performed every 30 min using a luminescence spectrophotometer.

2.6 ^{13}C CP MAS and ^{31}P liquid-state NMR spectroscopy measurements

Soil samples from the warming gradient were analyzed by ^{13}C CP MAS and liquid state ^{31}P NMR spectroscopy. The ^{13}C NMR spectra were acquired using a BRUKER DSX 200 NMR spectrometer (resonance frequency: 50.323 MHz, Bruker Corp. Rheinstetten, Germany). Samples were rotated at the magic angle (54.78°) with a spinning speed of 6.8 kHz to avoid line broadening due to orientation-dependent interactions (Wilson, 1987). We collected the spectra with a 700 ms pulse delay and used a ramped ^{1}H-pulse during a contact time of 1 ms to circumvent Hartmann-Hahn mismatches (Peersen et al., 1993). Depending on sample sensitivity, the number of accumulated scans ranged between 10,000 and 100,000. We used a line broadening between 10 and 15 Hz before Fourier transformation to improve the signal-to-noise ratio. The chemical shift is given relative to tetramethylsilane (0 ppm), calibrated with glycine (176.03 ppm). We used seven spectral integration regions: carbonyl-C (210–165 ppm), O-aromatic-C (165–145 ppm), aromatic-C (145–110 ppm), O_2-alkyl-C (110–95 ppm), O-alkyl-C (95–60 ppm), N-alkyl/methoxyl-C (60–45 ppm) and alkyl-C (45–10 ppm) (Nelson and Baldock, 2005).

The liquid state ^{31}P NMR spectroscopy, required an extraction of the soil samples using 0.25M NaOH and 0.05M EDTA for 16 h. Thereafter, the suspensions were centrifuged at 14,000g for 30 min (Vestergren et al., 2012) and the supernatants were frozen and lyophilized. For the NMR measurement, 100 mg of freeze-dried solids were dissolved in 500 µL of a mixture of NaOD and D_2O at pH 13, and 100 µL of methylene phosphonic acid (MDPA, 0.84 mg/mL in D_2O) was added as internal reference (Cade-Menun and Liu, 2013). Solution 1D ^{31}P NMR spectra were acquired on a Varian 600 MHz spectrometer equipped with a 5 mm broadband probe tuned to ^{31}P nucleus. The spectra were acquired with the following parameters: 45° pulse calibrated at 6.39 µs, 0.4 s acquisition time, 5 s relaxation delay, 15,800 scans, proton inverse-gated decoupling, at 293.15 K. For signal identification, a soil extract was analyzed with the 2D HSQC method. Total experimental time was 41.5 h, and ^{31}P decoupling was turned on during acquisition. 1D and 2D spectra were processed using MNOVA. Zero fillings were applied to boost resolution by extending to 4k and 1k data points in F2 and F1 dimensions.

2.7 Bulk XANES spectroscopy measurements

Synchrotron XANES spectra were acquired at different facilities and beamlines, according to the energy required. For instance, Soil C and N K-edge XANES spectra were acquired at the NIST U7A beamline of the National Synchrotron Light Source (NSLS) located at the Brookhaven National Laboratory, Upton, NY, USA. Samples were prepared as a fine-ground sample powder spread into a Cu tape mounted on a sample holder (12 h desiccation under vacuum). The spectra were acquired in Partial Electron Yield (PEY) mode using a channeltron electron multiplier with an entrance grid voltage of -50 V. The incident beam intensity at the sample, I_0, and at the monochromator, I_{ref}. were measured simultaneously using a clean gold mesh located upstream of the samples and carbon mesh (C XANES) or a TiN mesh (N XANES) upstream of the monochromator, respectively. For each sample, we acquired at least two spectra and no radiation damage was observed.

The P K-edge and L-edge XANES spectra were acquired at the SXS and PGM beamlines of the Brazilian Synchrotron Light Source (LNLS) located at the National Center for Research in Energy and Materials, Campinas, SP, Brazil. For the P K-edge XANES spectroscopy measurements, pellets were prepared of 13 mm diameter using 120 mg of each sample. Thereafter, the samples were mounted on a stainless-steel sample holder and covered with a 4 μm thin ultralene window film (Spex SamplePrep, Metuchen, NJ, USA). Samples and standards were mounted at the beamline and measured under vacuum. The detector was placed at a solid angle of 45° from the incident monochromatic beam to increase the fluorescence signal. The P $L_{2,3}$-edge XANES spectra were as acquired at the PGM beamline by spreading a thin layer of powder onto a double-sided P-free carbon tape "Spectro-tabs" (Catalog No. G3358, Plano GmbH, Wetzlar, Germany). Spectra acquisition was performed by recording the X-ray absorption as total electron yield (TEY) with an amperemeter. Recorded spectra were normalized to the incident beam intensity (I_0), which was simultaneously recorded as the absorption from a gold mesh upstream of the beamline.

Finally, S and some P spectra were acquired at Beamline-8 of the Synchrotron Light Research Institute (SLRI). Samples were spread as fine-ground powder on S-and P-free Kapton tape (Lanmar Inc., North Brook, IL, USA) and mounted on a sample holder. We calibrated the monochromator (InSb (1 1 1) double-crystal monochromator with an energy resolution of $\Delta E/E = 3 * 10^4$) every 12 h, using the sulfate white-line of $FeSO_4$ (2482.5 ± 0.11 eV) or elemental P (2145.5 eV).We summarize the parameters for data collection for all the elements in Table 3.

Table 3. Acquisition parameters for the C, N, P, S K-edge as well as the P $L_{2,3}$-edge XANES spectra.

Element	Energy (eV)	Step size (eV)	Dwell time (s)
C	270 – 340	0.25	1
N	380 – 450	0.25	1
P K-edge	2045.5 – 2105.5	5	3
	2105.5 – 2135.5	1	3
	2135.5 – 2195.5	0.25	3
	2195.5 – 2245.5	1	3
	2245.5 – 2495.5	5	3
P $L_{2,3}$-edge	130 – 160	0.1	1
S	2450 – 2465	1	3
	2465 – 2495	0.25	3
	2495 – 2530	1	3

Data analysis for the bulk XANES spectroscopy measurements followed different approaches depending on the element analyzed. The C K-edge XANES spectra were analyzed using Python and the lmfit package (Newville and Stensitzki, 2014). Data pre-treatment consisted in background subtraction (280 – 283 eV) and normalization (310 – 330 eV). Thereafter, the spectra were deconvoluted using 36 Gaussian curves fitted between 284 to 320 eV, with constraints of ±0.2 eV on the sigma, a centroid shift up to 293 eV of ±0.2 eV and 293 eV of ±1 eV (Le Guillou et al., 2018; Sedlmair et al., 2012). We calculated the relative proportions of (i) aromatic (284, 284.3, 284.6, 284.9, 285.4, 285.8 eV) (ii) ketone, phenol, nitrile (286.1, 286.5, 286.8 eV), (iii) aliphatic (287.4, 287.7 eV), (iv) amide (288.1 eV), (v) carboxyl (288.4 eV), (vi) alcohol (2894, 289.9 eV), and (vii) carbonyl (290.3 eV) C functional group signals by summing the height of the curves and normalizing its proportion to 100%. The relative contribution of each component together with the C and N content of the samples were used to estimate the relative abundance of the main organic groups (carbohydrate, protein, lignin, lipid, carbonyl, char), and to calculate the nominal oxidation state of carbon (NOS-C) through the Molecular Mixing Model (MMM) (Hockaday et al., 2009; Nelson and Baldock, 2005).

The N K-edge XANES spectra were background subtracted (390 – 395 eV) and normalized (425 – 435 eV) to an edge step of 1, and linear combination (LC) fitting analysis was performed using the LCF package of the R statistical package. We combined three sets of standards for LC fitting, one measured under the same conditions as the sample and the other two sets of standards available from the literature. The first set was composed of 8-

hydroxychinoline, ammonium chloride, guanine, chitin, glucosamine, cysteine, and calcium nitrate. The second set, available from the literature was composed of acridine, ethyl methoxycarbonyl pyridinium iodide, and histidine (Dynes et al., 2019). The third set was composed of heterocyclic amino acids, namely: hydroxyproline, proline, histidine, tryptophan, and glycine (Kaznacheyev et al., 2002). We summarized the results in four groups: Amino sugars (chitin and glucosamine), amino acids+NH_4 (cysteine, glycine, and ammonium chloride), 6.-membered rings (acridine, 8-hydroxyquinoline), and 5-membered rings (hydroxyproline, proline, tryptophan, histidine).

The XANES spectra acquired at the P K-edge were visually evaluated for inconsistencies (e.g., glitches, drifts, and noise) between replicates of the same spectra and merging of the scans. Thereafter, all spectra were E_0-calibrated to the zero crossing of the second derivative of the absorption for each sample. To estimate the range where self-absorption affects the linearity of the white line increase, we tested the correlation of total P content with the area of the XANES spectra from 2137 to 2186 eV, before normalization, for the mixture of standards. This was done by integrating the abovementioned range using the Simpson method for integration in R. For the quantification of P species through XANES spectroscopy we first applied a baseline subtraction (−36 to −15 eV) and normalization (+37 to +58 eV) across all samples and standards. These values were optimized using the LCF R package (Werner and Prietzel, 2015) using the ranges for pre-edge background subtraction: between −43 eV to −30 eV and −19 eV to −9 eV and normalization values: between +34 eV to +40 eV and +50 eV to +65 eV, with respect to E_0. Thereafter, the fitting results were ranked according to their respective R-factor, and the fit with the lowest R-factor was reported.

We quantified different S species by deconvoluting the S K-edge XANES spectra, using the software package ATHENA (Ravel and Newville, 2005). The spectra were baseline-corrected (2450–2465 eV) and edge-normalized (2485–2490 eV). Then, spectral deconvolution was performed with the Gaussian Curve Fitting method as described by Prietzel et al. (2011). We accounted for the S oxidation state dependency of the absorption cross-section (Xia et al., 1998), by multiplying the areas as calculated for the different Gaussian peaks with the respective correction factors (Prietzel et al., 2011). The contribution of each S species to total S was calculated by normalizing each corrected peak area to the sum of the corrected areas of all S species present in a sample.

2.8 Cryo and ambient temperature μ-XRF and μ-XANES measurements

Root samples of the calcareous soil variant from *Study 3* were analyzed by Cryo μ-XRF and μ-XANES at the PHOENIX beamline of the Swiss Light Source (SLS), while the samples from the silicate soil variant were analyzed at the I08 beamline of Diamond Light Source (DLS). Freshly harvested samples from the calcareous variant were kept humid using a humifier and sectioned to 100 μm thickness using two evenly spaced razor blades, and immediately after high-pressure frozen in aluminium planchets of 3 mm diameter. Samples from the silicate variant were additionally sectioned to 100 μm and mounted in TEM grids, without cryo-freezing.

The cryo-temperature measurements at the SLS were made using an in-house designed cryo-sample holder (Figure 7). The cryo-sample holder consisted of a copper block, with a small volume for liquid nitrogen to maintain the sample cold during transference and a flat surface where the high pressure frozen planchets could be attached under liquid nitrogen. During transference, the sample holder was screwed directly to a copper cold finger connected to a Dewar with liquid nitrogen, warranting that the sample holder temperature was constantly -176 °C. The chamber was vented with nitrogen to minimize humidity. After transference, a heater within the sample holder increased the sample temperature to -120 °C under vacuum, to etch the sample surface.

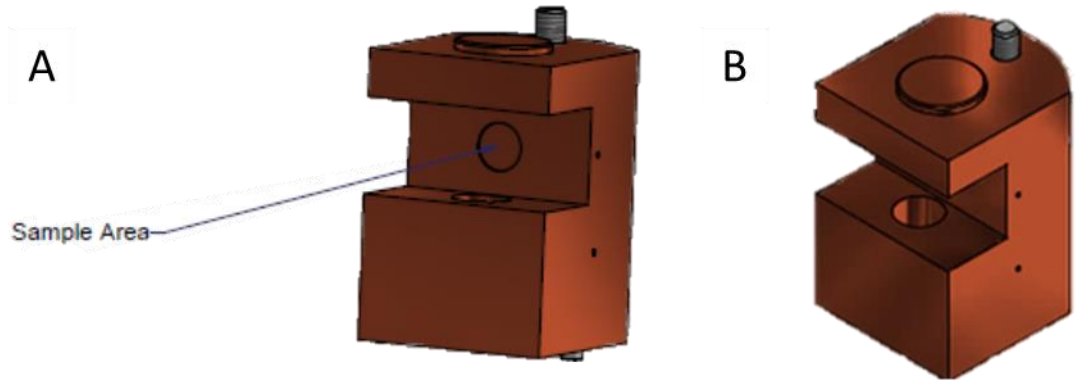

Figure 7. Cryo-sample holder designed for use at the PHOENIX beamline (SLS). (A) Side-view. (B) Top-view.

At the Phoenix beamline the focusing mirrors were tuned as to allow both the 1st and the 3rd harmonic of the source. Thereafter, a Si (111) DCM selected the energy of 2.4 keV (7.2 keV at the 3rd harmonic) as to allow simultaneous mapping of C, P, Ca, and Fe (flux: 10^{10} photons sec^{-}

[1]). The spot size was ~2 x 2 μm^2 and maps with a pixel size of 1 μm were produced. The μ-XRF and μ-XANES signals were collected using a single element SDD detector (Ketek GmbH, Germany). Meanwhile at the I08 beamline, the energy of 2.7 keV was selected using a PGM monochromator. The μ-XRF and μ-XANES signals were collected using a multi element SDD detector (Bruker GmbH, Germany), which allows the mapping of P and C, while simultaneously analyzing the L-edges of Ca and Fe. The spot size was ~0.6 μm and maps with a pixel size of 0.6 μm were produced. At both beamlines a full Energy Dispersive Spectrum (EDS) was recorded for each pixel of the XRF map, and the spectra were fit using the PyMCA freeware (Solé et al., 2007). Image analysis was performed using Fiji (Schindelin et al., 2012). Since the chemistry of interest takes place in the organic/loamy/clay phases of the investigated soils, the primary minerals (SiO_2: quartz) were masked out, as these minerals are unlikely to participate in important chemical reactions. The total P distribution was segmented in Fiji, and the area cover was computed over the Al, Fe, C and Ca. The μ-XANES spectra were analysed using the *LCF* R package (Werner and Prietzel, 2015).

2.9 Data analysis

In all studies I used the R statistical software (R Core Team, 2018), together with the packages 'ggplot', and 'stats' to compute averages, standard errors, and correlative analyses. Variation partitioning analyses were performed in *Study 2*, using the 'vegan' package to fit a model that best explained the molecular structure of each element using the combination of variables for temperature (soil temperature), microbial biomass (fungal and bacterial biomass), and microbial necromass (fungal and bacterial necromass).

3. Results and Discussion

This section aims to discuss and summarize the results of the studies performed throughout this thesis. We direct the reader to the publications accessible on-line and in the appendix for a detailed presentation of the results.

3.1 Effect of self-absorption on LCF results

A major concern of the scientific community is that LCF results obtained via P K-edge XANES spectroscopy using FY mode often are biased or distorted by self-absorption. Several recommendations exist to minimize or even correct it (Booth and Bridges, 2005; Hesterberg et al., 1999; Kruse et al., 2015), and while there are ranges and rules of thumb concerning critical P concentrations recommended (0.2 to 5%, w/w), so far no systematic study of this effect has addressed this issue in detail. Thus, the first important fact we tested was which range of concentration of P is not affected by self-absorption effects. By systematically analyzing standard mixtures of the same composition, but increasing P content, we could determine that the ideal upper limit for reliable (i.e. not self-absorption confounded) P K-edge XANES spectroscopy is 75 mmol P kg^{-1}. Furthermore, we also investigated the effect of performing LC fitting exercises using iteratively optimized background subtraction and normalization values (thereafter named solely "optimized") *vs.* using "non-optimized" background and normalization values.

The P speciation of these samples, together with serially diluted soil samples were obtained by non-optimized and optimized LCF. The use of non-optimized LCF workflows yielded results with a mean error >15%, while by using optimized background subtraction and normalization values, consistent results with <10% error can be obtained for samples with P concentrations up to 300 mmol P kg^{-1} (Figure 8). Using diluted soil samples, we show that the variation across different P concentrations decreases when a considerate portion of the P in the investigated samples is present as calcium phosphate, whose spectral features are at energies above the white line. Meanwhile, spectral features on the pre-edge like those of iron phosphates are particularly sensitive to self-absorption. Thus, we recommend that LCF analyses are performed only for samples with P concentrations <75 mmol kg^{-1} under unoptimized analysis or up to 300 mmol kg^{-1} when using optimized LCF algorithms.

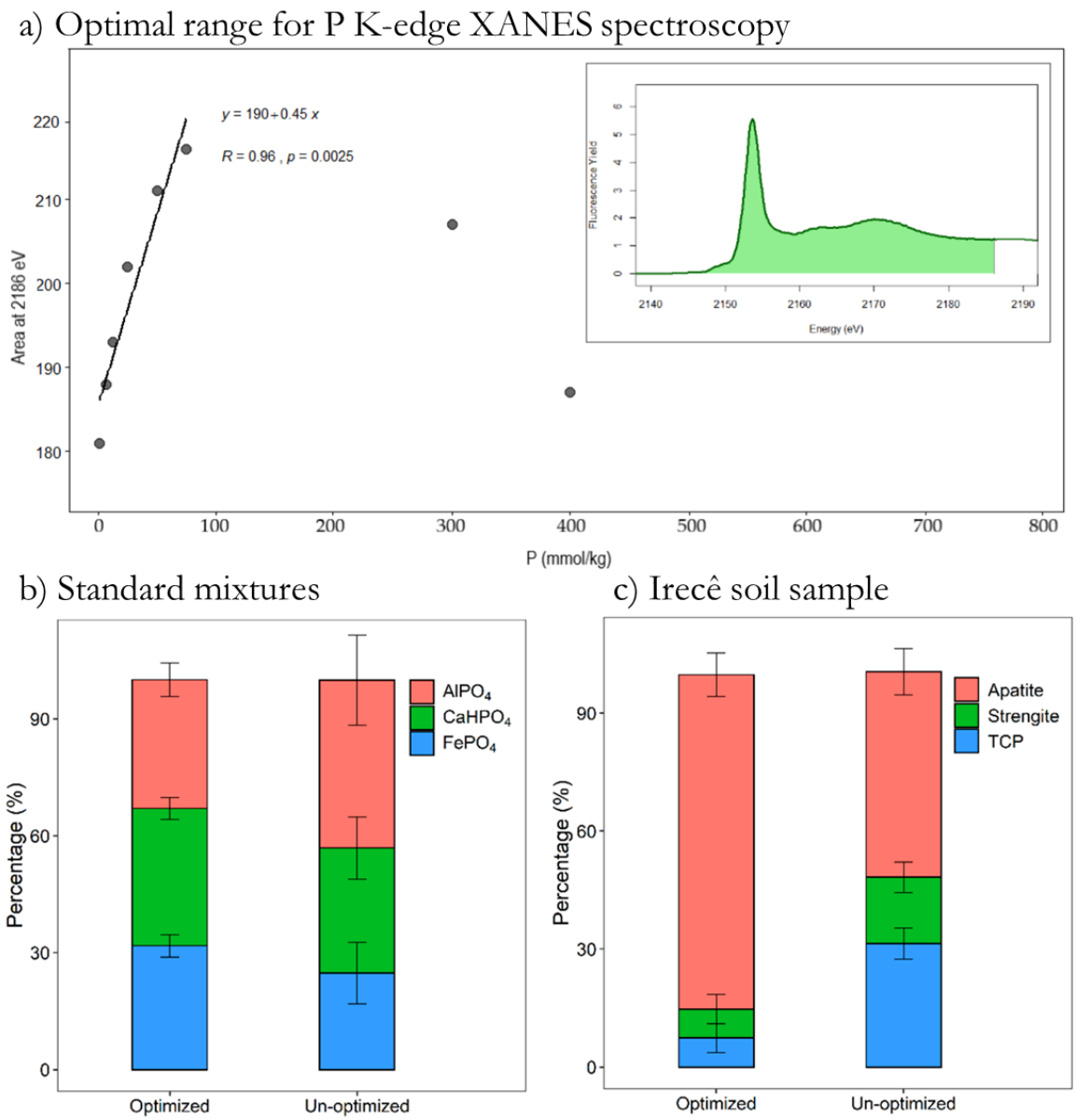

Figure 8. (a) Optimal range for P K-edge XANES spectroscopy and comparison between the LC fit results across the concentrations between 1 to 300 mmol P kg^{-1} on (b) the standard mixtures, and (c) the Irecê soil sample. TCP: Tricalcium phosphate.

3.2 A novel approach for P speciation using P L-edge XANES spectroscopy in soils and other environmental materials

Synchrotron-based methods provide a unique set of techniques that can reveal both the spatial distribution and speciation of P in soils and other environmental materials. However, the current approach using the K-edge of P does not provide sufficient resolution to distinguish different species of organic P (Kruse et al., 2009). Our study provides the first thorough analysis of the accuracy, precision, and P concentration necessary to analyze samples at the P $L_{2,3}$-edge. Using 40 standard mixtures we determined (Figure 9) that P $L_{2,3}$-edge XANES spectroscopy is capable of quantifying inorganic phosphates (Pearson correlation coefficient R measured *vs.* true P sample concentration between 0.84 and 0.93) and organic phosphates (R between 0.78 to 0.87). Our results also showed that with currently available detection systems and X-ray brilliance organic polyphosphates and diester phosphates are prone to underestimation. Furthermore, we determined that with currently available detector systems samples need to have P concentrations >3 mg g^{-1} to yield sufficient signal for TEY analyses. My work explores a new method for the speciation of P in soils and other environmental materials, and demonstrates that exploiting outer valence shells of P is a valuable tool to study phosphate compounds that barely distort the oxygen tetrahedra of the phosphate molecule. Other methods, like Resonant Inelastic X-ray Scattering (RIXS) and X-ray Raman Scattering (XRS) may also provide valuable information by exploring valence shell transitions of the phosphorus atom.

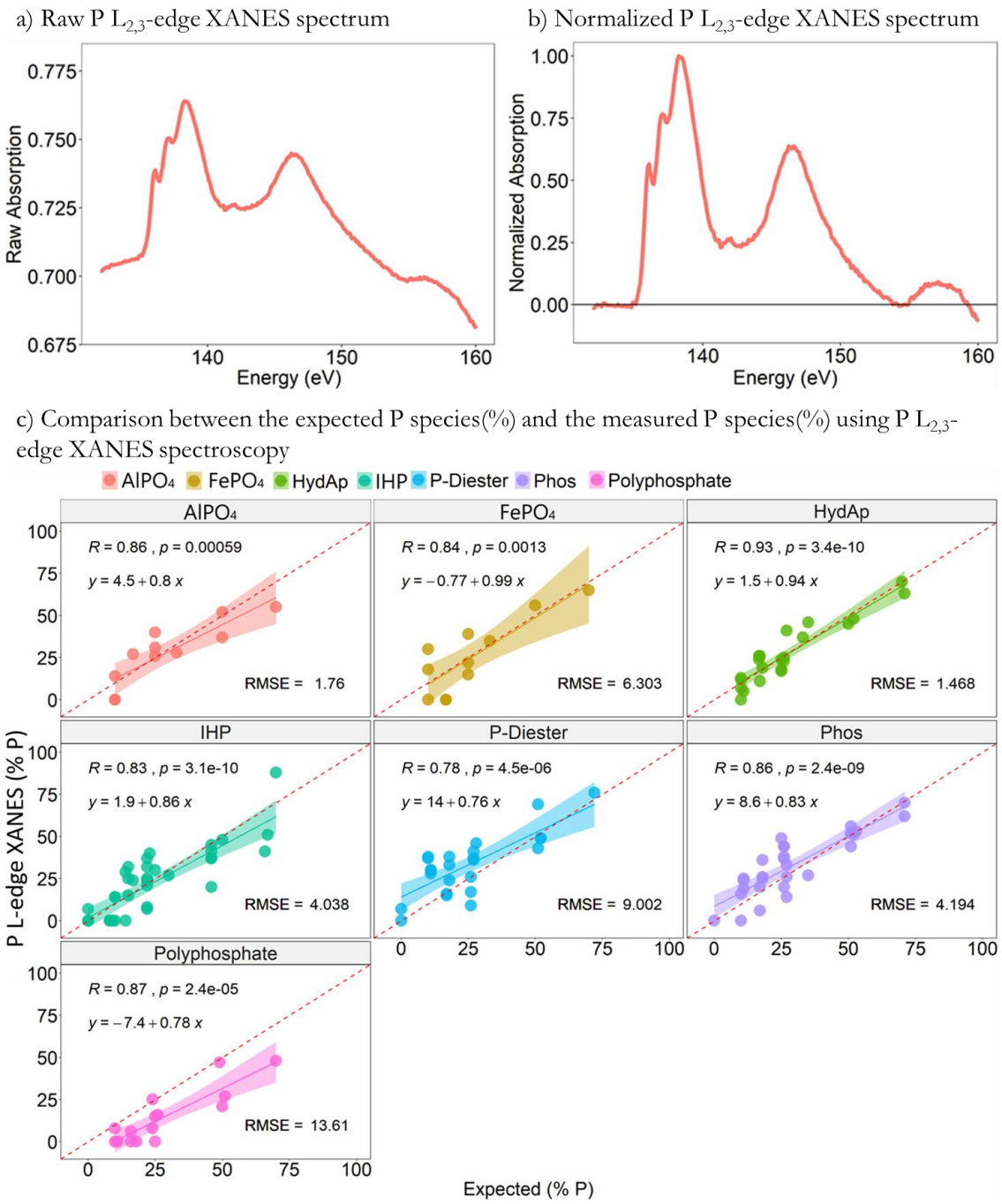

Figure 9. (a) P $L_{2,3}$-edge XANES spectrum of ATP diluted with quartz to a P concentration of 40 mg g^{-1} and (b) same spectrum after background subtraction and normalization. (c) Comparison of the contribution of different inorganic and organic P compounds in defined diluted (40 mg P g^{-1}) ternary and quaternary standard mixtures, as determined by P $L_{2,3}$-edge XANES spectroscopy with the true contribution of the respective compounds. Shown are linear regressions, with the shadowed area representing the 95% confidence interval. Pearson's correlation coefficients (R), p-values, and linear regression equations are printed in the upper left corner of each panel; the root-mean-square error (RMSE) is printed in the lower right corner of each panel.

3.3 Microbial community dynamics and SOM molecular diversity control soil carbon loss under warming

Temperate forests in mountainous regions are vulnerable to climate change, however, the shifts in the molecular composition of SOC and its associated elements (N, S, and P mainly) as consequence of increasing temperature and associated vegetation change at present still are unknown. Moreover, the change in microbial communities' composition and enzymatic activity patterns and link between these changes to the molecular composition of SOM and its associated elements are yet unexplored using state-of-the-art spectroscopic methods.

Here, using a temperature and vegetation gradient at two mountain forest sites in the German Alps, we observed that temperature increases are accompanied by lower SOC contents, yet no visible shifts in nutrient content. On the other hand, fungal biomass increased and the biomass of gram-negative bacteria decreased along the gradient. These shifts in microbial community composition were accompanied by decreases in phenol oxidase and acid monoesterphosphatase and increases in leucine peptidase activities. Our multi-spectroscopy data unravel the preferential depletion of lignin, amino peptides, and monoesterphosphates for the formation of microbial biomass and the accumulation of heterocyclic N, sulfate, and inorganic phosphate (Figure 10). These findings indicate that under increasing temperature and decreasing C input, microbial turnover in mountain forest soils increases, and the remaining communities are preferentially shifted towards those that thrive under strained C and nutrient input. Our study harmonizes the information between abiotic and biotic controls of SOM biogeochemistry, providing a framework to understand the long-term effects of warming and associated vegetation change in temperate mountain forests.

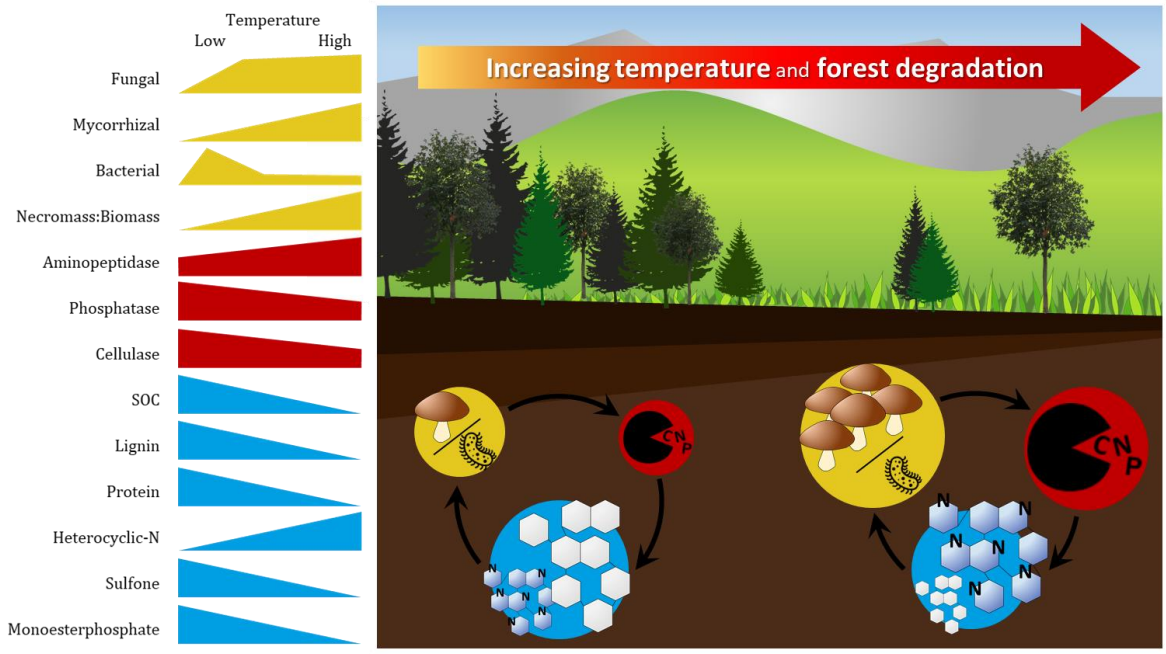

Figure 10. Conceptual schematic overview of the main soil changes along the temperature gradient related to the enzymatic specific activity, molecular SOM composition, and microbial community composition and trajectories of biochemical and microbial response to increasing temperature and forest degradation.

3.4 Functional root plasticity shapes patterns of phosphorus acquisition in temperate forests

Here, using *Picea abies* L. seedlings grown in mesocosms containing artificial soils with contrasting initial P speciation (organic or inorganic P) and mineral composition (silicate-derived or dolomite-derived), we observed that soils rich in inorganic P accumulate more C and allow more P acquisition than soils rich in organic P. These patterns were accompanied by changes in the root functional traits exhibited by the plants; for instance, roots of *Picea abies* L. seedlings grown in inorganic P-rich soils were thinner and longer than those of *Picea abies* L. seedlings grown in organic P-rich soils, thus making the former less prone to effective mycorrhization than the latter. At the microscale, P depletion at the root-soil interface was more pronounced in inorganic P-rich soils, while in organic P-rich soils the co-localization of P with C was higher. Our microscale analysis unravels the preferential mechanisms of plant P acquisition depending on soil P speciation, with root-microbial association and cooperation obviously being more important for soils rich in organic P than for soil rich in inorganic P. Furthermore, we reveal that this is accompanied by root functional shifts within the same species (Figure 11). These findings showcase the root functional plasticity that allows temperate forests to thrive under different P speciation conditions and to modulate different P acquisition mechanisms at the microscale.

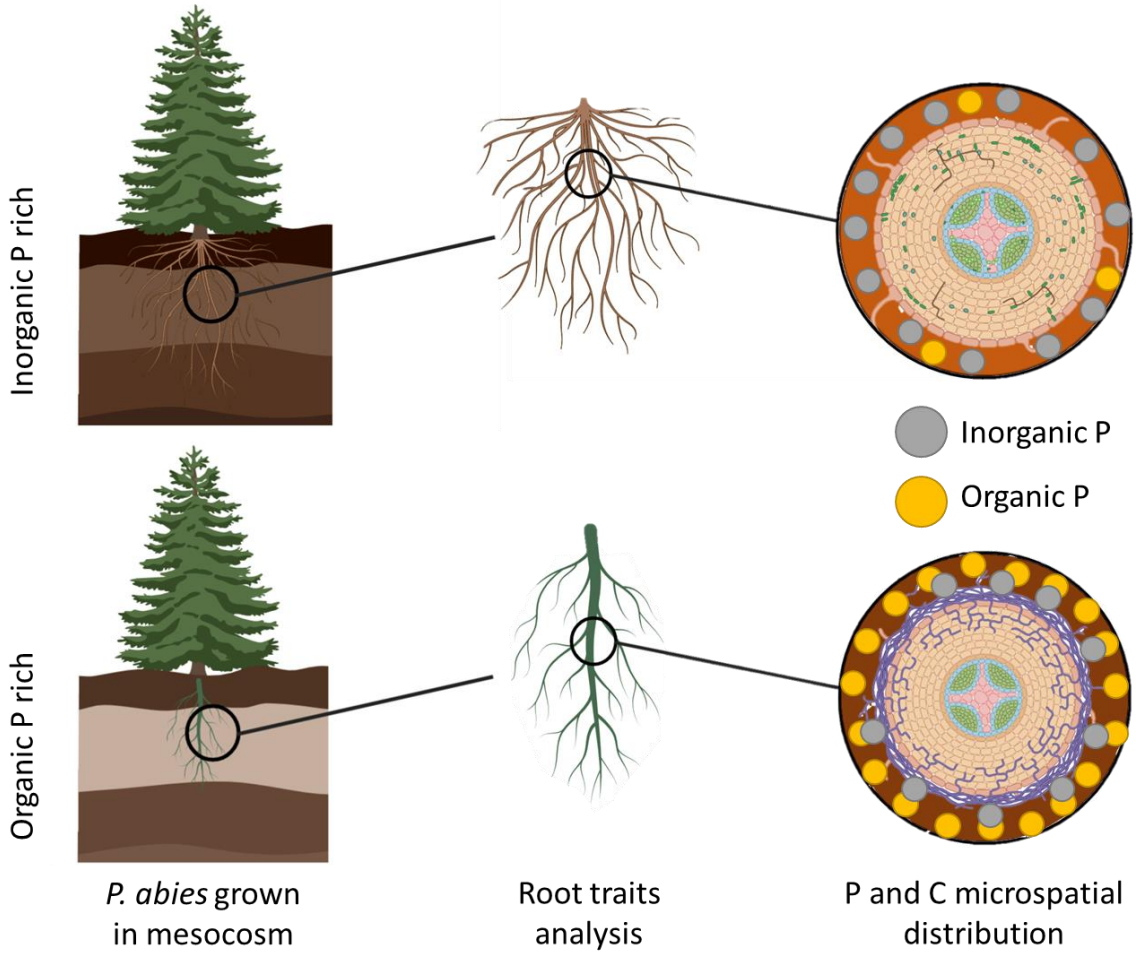

Figure 11. Picea abies L. root traits and microspatial P patterns driven by initial soil P speciation. Soil P speciation and availability shape plant investment in roots and soil microbiome: Plants grown in inorganic P-rich soils develop more branched and thinner roots while plants grown in organic P-rich soils develop thicker roots. The difference in root traits shapes the microspatial distribution of P at the root-soil interface, with organic P-rich soils having a higher co-localization of C with P than inorganic P-rich soils due to the microbially mediated organic P mineralization.

4. Conclusions and Outlook

This thesis improves our overall understanding of the P cycle in soils. I developed important methodological improvements for the speciation and analysis of P in soils at the macro- and the microscale. My studies demonstrated that accurate and precise bulk P K-edge XANES spectroscopy results can be obtained using optimized algorithms for LC fitting. I observed that these approaches yield consistent results across different soil P concentrations even when spectra are distorted by self-absorption. Therefore, I recommend applying such background and normalization optimization routines to yield a most correct quantification of different organic and inorganic P species in soils in future studies; moreover, a consistent P concentration across the samples is also recommended for better results. The latter can easily be achieved by appropriate sample dilution prior to analysis.

The findings in the temperature gradient study contribute to our overall comprehension of the influence of climate change on the shifts in soil OC, N, S, and P molecular composition. Concomitant with the soil C, N, P, and S speciation changes, additionally, fungal biomass increased and the biomass of gram-negative bacteria decreased along the gradient. We concluded that under increasing temperature and decreasing C input, microbial turnover increases, and the remaining communities are preferentially shifted towards those that thrive under strained C and nutrient input. This study shows the benefits of using multi-elemental spectroscopy and combining physico-chemical with microbiological analyses to assess the impact of abiotic and biotic disturbances in SOM biogeochemistry.

The microcosm experiment for the first time provides direct evidence of different pathways of tree P acquisition exhibited in temperate forests. By examining the different root functional traits exhibited in (otherwise identical) artificial soils with different initial P speciation, and relating them to microspatial soil P distribution patterns, I elucidated dominant processes of tree P acquisition in temperate forests depending on soil P speciation. Furthermore, my novel approach using cryo-microspectroscopy allows the joint analysis of microscale C and P distribution and speciation in soils, opening a window for novel studies that aim to investigate the relationship between C and nutrients.

While P K-edge XANES spectroscopy allows an accurate speciation of most P compounds in soils, our project showcases the importance of organic soil P compounds for P nutrition in temperate forests. Our approach using P $L_{2,3}$-edge XANES spectroscopy enables a more detailed speciation of organic P compounds, and has the potential to acquire more

detailed spatially resolved information based on direct, non-invasive measurements, on the organic P dynamics in soils.

Overall, this thesis explored the capabilities of synchrotron-based X-ray spectroscopy and microspectroscopy techniques for P speciation in soils at the macro- and the microscale, and highlighted the interrelation of spatial soil P speciation patterns with other physicochemical soil properties (e.g. soil structure, element composition, organo-mineral assemblage). The results of my studies can be extrapolated to other soils and materials, and provide a framework for future studies aiming to apply correlative analyses of different element speciation techniques.

5. Bibliography

Adediran, G.A., Tuyishime, J.R.M., Vantelon, D., Klysubun, W., Gustafsson, J.P., 2020. Phosphorus in 2D: Spatially resolved P speciation in two Swedish forest soils as influenced by apatite weathering and podzolization. Geoderma 376, 114550. doi:10.1016/j.geoderma.2020.114550

Angst, G., Messinger, J., Greiner, M., Häusler, W., Hertel, D., Kirfel, K., Kögel-Knabner, I., Leuschner, C., Rethemeyer, J., Mueller, C.W., 2018. Soil organic carbon stocks in topsoil and subsoil controlled by parent material, carbon input in the rhizosphere, and microbial-derived compounds. Soil Biology and Biochemistry 122, 19–30. doi:10.1016/j.soilbio.2018.03.026

Bardgett, R.D., Hobbs, P.J., Frostegård, Å., 1996. Changes in soil fungal:bacterial biomass ratios following reductions in the intensity of management of an upland grassland. Biology and Fertility of Soils 22, 261–264. doi:10.1007/BF00382522

Baumann, K., Siebers, M., Kruse, J., Eckhardt, K.U., Hu, Y., Michalik, D., Siebers, N., Kar, G., Karsten, U., Leinweber, P., 2019. Biological soil crusts as key player in biogeochemical P cycling during pedogenesis of sandy substrate. Geoderma 338, 145–158. doi:10.1016/j.geoderma.2018.11.034

Bennet, E., Elser, J., 2009. A broken biogeochemical cycle. Nature 478, 29–31. doi:10.1038/478029a

Bligh, E.G., Dyer, W.J., 1959. A Rapid Method of Total Lipid Extraction and Purification. Canadian Journal of Biochemistry and Physiology 37, 911–917. doi:10.1139/y59-099

Booth, C.H., Bridges, F., 2005. Improved SelfAbsorption Correction for Fluorescence Measurements of Extended XRay Absorption FineStructure. Physica Scripta 202. doi:10.1238/Physica.Topical.115a00202

Bouazza, A., Vangpaisal, T., Jefferis, S., 2006. Effect of Wet–Dry Cycles and Cation Exchange on Gas Permeability of Geosynthetic Clay Liners. Journal of Geotechnical and Geoenvironmental Engineering 132, 1011–1018. doi:10.1061/(asce)1090-0241(2006)132:8(1011)

Brookes, P.C., Powlson, D.S., Jenkinson, D.S., 1984. Phosphorus in the soil microbial biomass. Soil Biology and Biochemistry 16, 169–175. doi:10.1016/0038-0717(84)90108-

1

Bunker, G., 2010. Introduction to XAFS, Introduction to XAFS. doi:10.1017/cbo9780511809194

Cade-Menun, B.J., 2015. Improved peak identification in 31P-NMR spectra of environmental samples with a standardized method and peak library. Geoderma 257–258, 102–114. doi:10.1016/j.geoderma.2014.12.016

Cade-Menun, B.J., Liu, C.W., 2013. Solution Phosphorus-31 Nuclear Magnetic Resonance Spectroscopy of Soils from 2005 to 2013: A Review of Sample Preparation and Experimental Parameters. Soil Science Society of America Journal 78, 19. doi:10.2136/sssaj2013.05.0187dgs

Cade-Menun, B.J., Preston, C.M., 1996. A comparison of soil extraction procedures for 31P NMR spectroscopy. Soil Science. doi:10.1097/00010694-199611000-00006

Celi, L., Lamacchia, S., Barberis, E., 2000. Interaction of inositol phsophate with calcite. Nutrient Cycling in Agroecosystems 57, 271–277.

Chang, S.C., Jackson, M.L., 1958. Soil Phosphorus Fractions in Some Representative Soils. Journal of Soil Science 9, 109–119. doi:10.1111/j.1365-2389.1958.tb01903.x

Courtier-Murias, D., Farooq, H., Longstaffe, J.G., Kelleher, B.P., Hart, K.M., Simpson, M.J., Simpson, A.J., 2014. Cross polarization-single pulse/magic angle spinning (CPSP/MAS): A robust technique for routine soil analysis by solid-state NMR. Geoderma 226–227, 405–414. doi:10.1016/j.geoderma.2014.03.006

Doolette, A.L., Smernik, R.J., Dougherty, W.J., 2010. Rapid decomposition of phytate applied to a calcareous soil demonstrated by a solution 31P NMR study. European Journal of Soil Science 61, 563–575. doi:10.1111/j.1365-2389.2010.01259.x

Doolette, A.L., Smernik, R.J., Dougherty, W.J., 2011. Overestimation of the importance of phytate in NaOH-EDTA soil extracts as assessed by 31P NMR analyses. Organic Geochemistry 42, 955–964. doi:10.1016/j.orggeochem.2011.04.004

Dowling, N.J.E., Widdel, F., White, D.C., 1986. Phospholipid ester-linked fatty acid biomarkers of acetate-oxidizing sulphate-reducers and other sulphide-forming bacteria. Journal of General Microbiology 132, 1815–1825. doi:10.1099/00221287-132-7-1815

Dynes, J.J., Hook, J.M., Torres-Rojas, D., Regier, T.Z., Lehmann, J., Hestrin, R., Smernik,

R.J., Gillespie, A.W., 2019. Fire-derived organic matter retains ammonia through covalent bond formation. Nature Communications 10, 1–8. doi:10.1038/s41467-019-08401-z

Elser, J.J., 2012. Phosphorus: A limiting nutrient for humanity? Current Opinion in Biotechnology 23, 833–838. doi:10.1016/j.copbio.2012.03.001

Elser, J.J., Bracken, M.E.S., Cleland, E.E., Gruner, D.S., Harpole, W.S., Hillebrand, H., Ngai, J.T., Seabloom, E.W., Shurin, J.B., Smith, J.E., 2007. Global analysis of nitrogen and phosphorus limitation of primary producers in freshwater, marine and terrestrial ecosystems. Ecology Letters 10, 1135–1142. doi:10.1111/j.1461-0248.2007.01113.x

Federle, T.W., Livingston, R.J., Wolfe, L.E., White, D.C., 1986. A quantitative comparison of microbial community structure of estuarine sediments from microcosms and the field. Canadian Journal of Microbiology 32, 319–325. doi:10.1139/m86-063

Fendorf, S., Sparks, D.L., Lamble, G.M., Kelley, M.J., 1994. Applications of X-ray absorption fine structure spectroscopy to soils. Soil Science Society of America Journal 58, 1583–1595. doi:10.2136/sssaj1994.03615995005800060001x

Fleischer, K., Rammig, A., De Kauwe, M.G., Walker, A.P., Domingues, T.F., Fuchslueger, L., Garcia, S., Goll, D.S., Grandis, A., Jiang, M., Haverd, V., Hofhansl, F., Holm, J.A., Kruijt, B., Leung, F., Medlyn, B.E., Mercado, L.M., Norby, R.J., Pak, B., von Randow, C., Quesada, C.A., Schaap, K.J., Valverde-Barrantes, O.J., Wang, Y.-P., Yang, X., Zaehle, S., Zhu, Q., Lapola, D.M., 2019. Amazon forest response to CO2 fertilization dependent on plant phosphorus acquisition. Nature Geoscience. doi:10.1038/s41561-019-0404-9

Floch, C., Alarcon-Gutiérrez, E., Criquet, S., 2007. ABTS assay of phenol oxidase activity in soil. Journal of Microbiological Methods 71, 319–324. doi:10.1016/j.mimet.2007.09.020

Frostegård, Å., Tunlid, A., Bååth, E., 1993. Phospholipid Fatty Acid Composition, Biomass, and Activity of Microbial Communities from Two Soil Types Experimentally Exposed to Different Heavy Metals. Applied and Environmental Microbiology 59, 3605–3617. doi:10.1128/AEM.59.11.3605-3617.1993

Garcia Arredondo, M., Lawrence, C.R., Schulz, M.S., Tfaily, M.M., Kukkadapu, R., Jones, M.E., Boye, K., Keiluweit, M., 2019. Root-driven weathering impacts on mineral-organic associations in deep soils over pedogenic time scales. Geochimica et

Cosmochimica Acta 263, 68–84. doi:10.1016/j.gca.2019.07.030

Gérard, F., 2016. Clay minerals, iron/aluminum oxides, and their contribution to phosphate sorption in soils - A myth revisited. Geoderma 262, 213–226. doi:10.1016/j.geoderma.2015.08.036

Goulon, J., Goulon-Ginet, C., Cortes, R., Dubois, J.M., 1982. On experimental attenuation factors of the amplitude of the EXAFS oscillations in absorption, reflectivity and luminescence measurements. Journal de Physique 43, 539–548. doi:10.1051/jphys:01982004303053900

Graham, W.F., Duce, R.A., 1979. Atmospheric pathways of the phosphorus cycle. Geochimica et Cosmochimica Acta 43, 1195–1208. doi:10.1016/0016-7037(79)90112-1

Hedlund, K., 2002. Soil microbial community structure in relation to vegetation management on former agricultural land. Soil Biology and Biochemistry 34, 1299–1307. doi:10.1016/S0038-0717(02)00073-1

Hesterberg, D., 2010. Macroscale Chemical Properties and X-Ray Absorption Spectroscopy of Soil Phosphorus, Developments in Soil Science. Elsevier Masson SAS. doi:10.1016/S0166-2481(10)34011-6

Hesterberg, D., McNulty, I., Thieme, J., 2017. Speciation of Soil Phosphorus Assessed by XANES Spectroscopy at Different Spatial Scales. Journal of Environment Quality 46, 1190. doi:10.2134/jeq2016.11.0431

Hesterberg, D., Zhou, W., Hutchison, K.J., Beauchemin, S., Sayers, D.E., 1999. XAFS study of adsorbed and mineral forms of phosphate. Journal of Synchrotron Radiation 6, 636–638. doi:10.1107/S0909049599000370

Hinsinger, P., 2001. Bioavailability of soil inorganic P in the rhizosphere as affected by root-induced chemical changes: A review. Plant and Soil 237, 173–195. doi:10.1023/A:1013351617532

Hinsinger, P., Bengough, A.G., Vetterlein, D., Young, I.M., 2009. Rhizosphere: Biophysics, biogeochemistry and ecological relevance. Plant and Soil 321, 117–152. doi:10.1007/s11104-008-9885-9

Hinsinger, P., Plassard, C., Tang, C., Jaillard, B., 2003. Origins of root-mediated pH changes in the rhizosphere and their responses to environmental constraints: A review. Plant

and Soil 248, 43–59. doi:10.1023/A:1022371130939

Hockaday, W.C., Masiello, C.A., Randerson, J.T., Smernik, R.J., Baldock, J.A., Chadwick, O.A., Harden, J.W., 2009. Measurement of soil carbon oxidation state and oxidative ratio by 13C nuclear magnetic resonance. Journal of Geophysical Research: Biogeosciences 114, 1–14. doi:10.1029/2008JG000803

IUPAC, 2014. IUPAC Compendium of Chemical Terminology, in: IUPAC Compendium of Chemical Terminology. IUPAC, Research Triagle Park, NC. doi:10.1351/goldbook.I03352

Jenny, H., 1941. Factors of soil formation. A system of quantitative pedology, Geoderma. doi:10.1016/0016-7061(95)90014-4

Joergensen, R.G., 1996. The fumigation-extraction method to estimate soil microbial biomass: Calibration of the kEC value. Soil Biology and Biochemistry. doi:10.1016/0038-0717(95)00102-6

Jonard, M., Fürst, A., Verstraeten, A., Thimonier, A., Timmermann, V., Potočić, N., Waldner, P., Benham, S., Hansen, K., Merilä, P., Ponette, Q., de la Cruz, A.C., Roskams, P., Nicolas, M., Croisé, L., Ingerslev, M., Matteucci, G., Decinti, B., Bascietto, M., Rautio, P., 2015. Tree mineral nutrition is deteriorating in Europe. Global Change Biology 21, 418–430. doi:10.1111/gcb.12657

Kaznacheyev, K., Osanna, A., Jacobsen, C., Plashkevych, O., Vahtras, O., Ågren, H., Carravetta, V., Hitchcock, A.P., 2002. Innershell absorption spectroscopy of amino acids. Journal of Physical Chemistry A 106, 3153–3168. doi:10.1021/jp013385w

Kelly, S.D., Hesterberg, D., Ravel, B., 2008. Analysis of Soils and Minerals Using X-ray Absorption Spectroscopy, in: Methods of Soil Analysis Part 5—Mineralogical Methods. pp. 387–464. doi:10.2136/sssabookser5.5.c14

Kögel-Knabner, I., 2000. Analytical approaches for characterizing soil organic matter. Organic Geochemistry 31, 609–625. doi:10.1016/S0146-6380(00)00042-5

Koleva, I.I., Van Beek, T.A., Linssen, J.P.H., De Groot, A., Evstatieva, L.N., 2002. Screening of plant extracts for antioxidant activity: A comparative study on three testing methods. Phytochemical Analysis 13, 8–17. doi:10.1002/pca.611

Kruse, J., Abraham, M., Amelung, W., Baum, C., Bol, R., Kühn, O., Lewandowski, H.,

Niederberger, J., Oelmann, Y., Rüger, C., Santner, J., Siebers, M., Siebers, N., Spohn, M., Vestergren, J., Vogts, A., Leinweber, P., 2015. Innovative methods in soil phosphorus research: A review. Journal of Plant Nutrition and Soil Science 178, 43–88. doi:10.1002/jpln.201400327

Kruse, J., Leinweber, P., Eckhardt, K.U., Godlinski, F., Hu, Y., Zuin, L., 2009. Phosphorus L2,3-edge XANES: Overview of reference compounds. Journal of Synchrotron Radiation 16, 247–259. doi:10.1107/S0909049509000211

Lang, F., Bauhus, J., Frossard, E., George, E., Kaiser, K., Kaupenjohann, M., Krüger, J., Matzner, E., Polle, A., Prietzel, J., Rennenberg, H., Wellbrock, N., 2016. Phosphorus in forest ecosystems: New insights from an ecosystem nutrition perspective. Journal of Plant Nutrition and Soil Science 179, 129–135. doi:10.1002/jpln.201500541

Le Guillou, C., Bernard, S., De La Pena, F., Le Brech, Y., 2018. XANES-Based Quantification of Carbon Functional Group Concentrations. Analytical Chemistry 90, 8379–8386. doi:10.1021/acs.analchem.8b00689

Lehmann, J., Solomon, D., Kinyangi, J., Dathe, L., Wirick, S., Jacobsen, C., 2008. Spatial complexity of soil organic matter forms at nanometre scales. Nature Geoscience 1, 238–242. doi:10.1038/ngeo155

Leontowich, A.F.G., Hitchcock, A.P., Egerton, R.F., 2016. Radiation damage yields across the carbon 1s excitation edge. Journal of Electron Spectroscopy and Related Phenomena 206, 58–64. doi:10.1016/j.elspec.2015.11.010

Liang, C., Amelung, W., Lehmann, J., Kästner, M., 2019. Quantitative assessment of microbial necromass contribution to soil organic matter. Global Change Biology 25, 3578–3590. doi:10.1111/gcb.14781

Liang, C., Read, H.W., Balser, T.C., 2012. GC-based detection of aldononitrile acetate derivatized glucosamine and muramic acid for microbial residue determination in soil. Journal of Visualized Experiments 2–7. doi:10.3791/3767

Lindsay, W.L., 1979. Chemical equilibria in soils. John Wiley and Sons Ltd., Chichester, Sussex.

Mao, J., Cao, X., Olk, D.C., Chu, W., Schmidt-Rohr, K., 2017. Advanced solid-state NMR spectroscopy of natural organic matter. Progress in Nuclear Magnetic Resonance Spectroscopy 100, 17–51. doi:10.1016/j.pnmrs.2016.11.003

Marx, M.C., Wood, M., Jarvis, S.C., 2001. A microplate fluorimetric assay for the study of enzyme diversity in soils. Soil Biology and Biochemistry 33, 1633–1640. doi:10.1016/S0038-0717(01)00079-7

Mottana, A., 2004. X-ray absorption spectroscopy in mineralogy: Theory and Experiments in the XANES region, in: Spectroscopic Methods in Mineralogy. Eötvös University Press, Budapest. doi:10.1180/emu-notes.6.12

Nelson, P.N., Baldock, J.A., 2005. Estimating the molecular composition of a diverse range of natural organic materials from solid-state 13 C NMR and elemental analyses. Biogeochemistry 72, 1–34. doi:10.1007/s10533-004-0076-3

Newville, M., Stensitzki, T., 2014. Non-Linear Least-Squares Minimization and Curve-Fitting for Python. doi:10.5281/zenodo.11813

Ngosong, C., Gabriel, E., Ruess, L., 2012. Use of the Signature Fatty Acid 16:1 ω 5 as a Tool to Determine the Distribution of Arbuscular Mycorrhizal Fungi in Soil . Journal of Lipids 2012, 1–8. doi:10.1155/2012/236807

O'Day, P.A., Nwosu, U.G., Barnes, M.E., Hart, S.C., Berhe, A.A., Christensen, J.N., Williams, K.H., 2020. Phosphorus Speciation in Atmospherically Deposited Particulate Matter and Implications for Terrestrial Ecosystem Productivity. Environmental Science & Technology 54, 4984–4994. doi:10.1021/acs.est.9b06150

Okin, G.S., Mahowald, N., Chadwick, O.A., Artaxo, P., 2004. Impact of desert dust on the biogeochemistry of phosphorus in terrestrial ecosystems. Global Biogeochemical Cycles 18. doi:10.1029/2003GB002145

Peersen, O.B., Wu, X., Kustanovich, I., Smith, S.O., 1993. Variable-amplitude cross-polarization MAS NMR. Journal of Magnetic Resonance - Series A. doi:10.1006/jmra.1993.1231

Phillips, B.L., Zhang, Z., Kubista, L., Frisia, S., Borsato, A., 2016. NMR spectroscopic study of organic phosphate esters coprecipitated with calcite. Geochimica et Cosmochimica Acta 183, 46–62. doi:10.1016/j.gca.2016.03.022

Prietzel, J., 2020. Soil Phosphorus Heterogeneity Improves Growth and P Nutrition of Norway Spruce Seedlings. Frontiers in Forests and Global Change 3. doi:10.3389/ffgc.2020.00059

Prietzel, J., Ammer, C., 2008. Montane bergmischwälder der Bayerischen Kalkalpen: Reduktion der schalenwilddichte steigert nicht nur den verjüngungserfolg, sondern auch die bodenfruchtbarkeit. Allgemeine Forst- Und Jagdzeitung 179, 104–112.

Prietzel, J., Botzaki, A., Tyufekchieva, N., Brettholle, M., Thieme, J., Klysubun, W., 2011. Sulfur Speciation in Soil by S K -Edge XANES Spectroscopy: Comparison of Spectral Deconvolution and Linear Combination Fitting. Environmental Science & Technology 45, 2878–2886. doi:10.1021/es102180a

Prietzel, J., Christophel, D., 2014. Organic carbon stocks in forest soils of the German alps. Geoderma 221–222, 28–39. doi:10.1016/j.geoderma.2014.01.021

Prietzel, J., Falk, W., Reger, B., Uhl, E., Pretzsch, H., Zimmermann, L., 2020. Half a century of Scots pine forest ecosystem monitoring reveals long-term effects of atmospheric deposition and climate change. Global Change Biology 1–20. doi:10.1111/gcb.15265

Prietzel, J., Harrington, G., Häusler, W., Heister, K., Werner, F., Klysubun, W., 2016. Reference spectra of important adsorbed organic and inorganic phosphate binding forms for soil P speciation using synchrotron-based K-edge XANES spectroscopy. Journal of Synchrotron Radiation 23, 532–544. doi:10.1107/S1600577515023085

Prietzel, J., Prater, I., Colocho Hurtarte, L.C., Hrbáček, F., Klysubun, W., Mueller, C.W., 2019. Site conditions and vegetation determine phosphorus and sulfur speciation in soils of Antarctica. Geochimica et Cosmochimica Acta 246, 339–362. doi:10.1016/j.gca.2018.12.001

R Core Team, 2018. R: A language and environment for statistical computing. R Foundation for Statistical Computing. Vienna, Austria. doi:10.1108/eb003648

Rajan, S.S.S., 1975. Adsorption of divalent phosphate on hydrous aluminium oxide. Nature 253, 434–436. doi:10.1038/253434a0

Ravel, B., Newville, M., 2005. ATHENA, ARTEMIS, HEPHAESTUS: Data analysis for X-ray absorption spectroscopy using IFEFFIT. Journal of Synchrotron Radiation 12, 537–541. doi:10.1107/S0909049505012719

Refshauge, S., Watt, M., McCully, M.E., Huang, C.X., 2006. Frozen in time: A new method using cryo-scanning electron microscopy to visualize root-fungal interactions: Methods. New Phytologist 172, 369–374. doi:10.1111/j.1469-8137.2006.01825.x

Rehr, J.J., Albers, R.C., 2000. Theoretical approaches to x-ray absorption fine structure. Reviews of Modern Physics 72, 621–654. doi:10.1103/RevModPhys.72.621

Rehr, J.J., Ankudinov, A., Zabinsky, S.I., 1998. New developments in NEXAFS/EXAFS theory. Catalysis Today 39, 263–269. doi:10.1016/S0920-5861(97)00109-0

Ruess, L., Chamberlain, P.M., 2010. The fat that matters: Soil food web analysis using fatty acids and their carbon stable isotope signature. Soil Biology and Biochemistry 42, 1898–1910. doi:10.1016/j.soilbio.2010.07.020

Saunders, W.M.H., Williams, E.G., 1955. Observations on the Determination of Total Organic Phosphorus in Soils. Journal of Soil Science 6, 254–267. doi:10.1111/j.1365-2389.1955.tb00849.x

Schindelin, J., Arganda-Carreras, I., Frise, E., Kaynig, V., Longair, M., Pietzsch, T., Preibisch, S., Rueden, C., Saalfeld, S., Schmid, B., Tinevez, J.Y., White, D.J., Hartenstein, V., Eliceiri, K., Tomancak, P., Cardona, A., 2012. Fiji: An open-source platform for biological-image analysis. Nature Methods. doi:10.1038/nmeth.2019

Schwertmann, U., Cornell, R.M., 1993. Iron Oxides in Laboratory. Soil Science. doi:10.1097/00010694-199311000-00012

Sedlmair, J., Gleber, S.C., Peth, C., Mann, K., Niemeyer, J., Thieme, J., 2012. Characterization of refractory organic substances by NEXAFS using a compact X-ray source. Journal of Soils and Sediments 12, 24–34. doi:10.1007/s11368-011-0385-9

Smernik, R.J., Doolette, A.L., Noack, S.R., 2015. Identification of RNA Hydrolysis Products in NaOH-EDTA Extracts using 31P NMR Spectroscopy. Communications in Soil Science and Plant Analysis 46, 2746–2756. doi:10.1080/00103624.2015.1093640

Smernik, R.J., Dougherty, W.J., 2007. Identification of Phytate in Phosphorus-31 Nuclear Magnetic Resonance Spectra: The Need for Spiking. Soil Science Society of America Journal 71, 1045–1050. doi:10.2136/sssaj2006.0295

Soil Survey Staff, 1999. Soil Taxonomy: A Basic System of Soil Classification for Making and Interpreting Soil Surveys., 2nd editio. ed, Agriculture Handbook No. 436.

Solé, V.A., Papillon, E., Cotte, M., Walter, P., Susini, J., 2007. A multiplatform code for the analysis of energy-dispersive X-ray fluorescence spectra. Spectrochimica Acta - Part B Atomic Spectroscopy 62, 63–68. doi:10.1016/j.sab.2006.12.002

Stemmer, M., Gerzabek, M.H., Kandeler, E., 1998. Organic matter and enzyme activity in particle-size fractions of soils obtained after low-energy sonication. Soil Biology and Biochemistry 30, 9–17. doi:10.1016/S0038-0717(97)00093-X

Torrent, J., Schwertmann, U., Barrón, V., 1992. Fast and slow phosphate sorption by goethite-rich natural materials. Clays and Clay Minerals 40, 14–21. doi:10.1346/CCMN.1992.0400103

Trevorah, R.M., Chantler, C.T., Schalken, M.J., 2019. Solving self-absorption in fluorescence. IUCrJ 6, 1–17. doi:10.1107/s2052252519005128

Tröger, L., Arvanitis, D., Baberschke, K., Michaelis, H., Grimm, U., Zschech, E., 1992. Full correction of the self-absorption in soft-fluorescence extended x-ray-absorption fine structure. Physical Review B 46, 3283–3289. doi:10.1103/PhysRevB.46.3283

Turner, B.L., 2008a. Resource partitioning for soil phosphorus: A hypothesis. Journal of Ecology 96, 698–702. doi:10.1111/j.1365-2745.2008.01384.x

Turner, B.L., 2008b. Soil organic phosphorus in tropical forests: An assessment of the NaOH-EDTA extraction procedure for quantitative analysis by solution 31P NMR spectroscopy. European Journal of Soil Science 59, 453–466. doi:10.1111/j.1365-2389.2007.00994.x

Turner, B.L., Brenes-Arguedas, T., Condit, R., 2018. Pervasive phosphorus limitation of tree species but not communities in tropical forests. Nature 555, 367–370. doi:10.1038/nature25789

Turner, B.L., Cade-Menun, B.J., Condron, L.M., Newman, S., 2005. Extraction of soil organic phosphorus. Talanta 66, 294–306. doi:10.1016/j.talanta.2004.11.012

van Veelen, A., Koebernick, N., Scotson, C.S., McKay-Fletcher, D., Huthwelker, T., Borca, C.N., Mosselmans, J.F.W., Roose, T., 2019. Root-induced soil deformation influences Fe, S and P: rhizosphere chemistry investigated using synchrotron XRF and XANES, New Phytologist. doi:10.1111/nph.16242

Vestergren, J., Vincent, A.G., Jansson, M., Persson, P., Ilstedt, U., Gröbner, G., Giesler, R., Schleucher, J., 2012. High-resolution characterization of organic phosphorus in soil extracts using 2D 1H-31P NMR correlation spectroscopy. Environmental Science & Technology 46, 3950–3956. doi:10.1021/es204016h

Vincent, A.G., Schleucher, J., Gröbner, G., Vestergren, J., Persson, P., Jansson, M., Giesler, R., 2012. Changes in organic phosphorus composition in boreal forest humus soils: the role of iron and aluminium. Biogeochemistry 108, 485–499. doi:10.1007/s10533-011-9612-0

Vincent, A.G., Vestergren, J., Gröbner, G., Persson, P., Schleucher, J., Giesler, R., 2013. Soil organic phosphorus transformations in a boreal forest chronosequence. Plant and Soil 367, 149–162. doi:10.1007/s11104-013-1731-z

Walker, T.W., Syers, J.K., 1976. The fate of phosphorus during pedogenesis. Geoderma 15, 1–19. doi:10.1016/0016-7061(76)90066-5

Wan, B., Yan, Y., Liu, F., Tan, W., Chen, X., Feng, X., 2016. Surface adsorption and precipitation of inositol hexakisphosphate on calcite: A comparison with orthophosphate. Chemical Geology 421, 103–111. doi:10.1016/j.chemgeo.2015.12.004

Wang, L., Amelung, W., Prietzel, J., Willbold, S., 2019. Transformation of organic phosphorus compounds during 1500 years of organic soil formation in Bavarian Alpine forests – A 31P NMR study. Geoderma 340, 192–205. doi:10.1016/j.geoderma.2019.01.029

Werner, F., Mueller, C.W., Thieme, J., Gianoncelli, A., Rivard, C., Höschen, C., Prietzel, J., 2017. Micro-scale heterogeneity of soil phosphorus depends on soil substrate and depth. Scientific Reports 7, 1–9. doi:10.1038/s41598-017-03537-8

Werner, F., Prietzel, J., 2015. Standard Protocol and Quality Assessment of Soil Phosphorus Speciation by P K-Edge XANES Spectroscopy. Environmental Science & Technology 49, 10521–10528. doi:10.1021/acs.est.5b03096

White, D.C., Davis, W.M., Nickels, J.S., King, J.D., Bobbie, R.J., 1979. Determination of the sedimentary microbial biomass by extractible lipid phosphate. Oecologia 40, 51–62. doi:10.1007/BF00388810

Willmott, P., 2019. An introduction to synchrotron radiation: Techniques and applications, An introduction to synchrotron radiation: Techniques and applications. Wiley. doi:10.1002/9781119280453

Wilson, M.A., 1987. NMR Techniques & Applications in Geochemistry & Soil Chemistry. Pergamon, Amsterdam. doi:10.1016/C2009-0-11075-9

Xia, K., Weesner, F., Bleam, W.F., Helmke, P.A., Bloom, P.R., Skyllberg, U.L., 1998. XANES Studies of Oxidation States of Sulfur in Aquatic and Soil Humic Substances. Soil Science Society of America Journal 62, 1240–1246. doi:10.2136/sssaj1998.03615995006200050014x

Yan, Y., Li, W., Yang, J., Zheng, A., Liu, F., Feng, X., Sparks, D.L., 2014. Mechanism of myo-inositol hexakisphosphate sorption on amorphous aluminum hydroxide: Spectroscopic evidence for rapid surface precipitation. Environmental Science & Technology 48, 6735–6742. doi:10.1021/es500996p

Yan, Y.P., Liu, F., Li, W., Liu, F., Feng, X.H., Sparks, D.L., 2014. Sorption and desorption characteristics of organic phosphates of different structures on aluminium (oxyhydr)oxides. European Journal of Soil Science 65, 308–317. doi:10.1111/ejss.12119

Zhang, X., Amelung, W., 1996. Gas chromatograph1c determination of muramic acid, glucosamine, mannosamine, and galactosamine in soils. Soil Biology and Biochemistry 28, 1201–1206. doi:10.1016/0038-0717(96)00117-4

Zhang, X., Dippold, M.A., Kuzyakov, Y., Razavi, B.S., 2019. Spatial pattern of enzyme activities depends on root exudate composition. Soil Biology and Biochemistry 133, 83–93. doi:10.1016/j.soilbio.2019.02.010

Appendix

Appendix 1	
Title	Optimization of Data Processing Minimizes Impact of Self-Absorption on phosphorus Speciation Results by P K-Edge XANES
Authors	**Colocho Hurtarte, L.C.**, Souza-Filho, L.F., Santos, W.O., Vergütz, L., Prietzel, J., Hesterberg, D.
Publication	Soil Systems 3 (2019), 61. 10.3390/soilsystems3030061

Appendix 2	
Title	A Novel Approach for the Quantification of Different Inorganic and Organic Phosphorus Compounds in Environmental Samples by P $L_{2,3}$ -Edge X-ray Absorption Near-Edge Structure (XANES) Spectro-scopy
Authors	**Colocho Hurtarte, L.C**., Santana Amorim, H.C., Kruse, J., Criginski Cezar, J., Klysubun, W., Prietzel, J.
Publication	Environmental Science & Technology 54 (2020) 2812-2820. 10.1021/acs.est.9b07018

Appendix 3	
Title	Quantifying Molecular-level Soil Organic Matter Changes in Temperate Mixed Mountain Forests in Response to Climate Warming
Authors	**Colocho Hurtarte, L.C.,** Mueller, S., Wang, L., Kandeler, E., Amelung, W., Willbold, S., Thieme, J., Jaye, C., Fischer, D., Klysubun, W., Prietzel, J.
Publication	In preparation

Appendix 4	
Title	Functional plasticity shapes patterns of phosphorus acquisition in temperate forests
Authors	**Colocho Hurtarte L. C.** , Liao D., Schweizer S., Müller S., Araki T., Wetter R. , Borca C., Huthwelker T., Klingl A., Prietzel J.
Publication	In preparation